Hydrothermal Aging of Fire-Protective Fabrics

Md. Saiful Hoque[1], Ankit Saha[2], Hyun-Joong Chung[2], and Patricia I. Dolez[1*]

[1]Department of Human Ecology, University of Alberta, T6G 2R3, Canada
[2]Department of Chemical and Materials Engineering, University of Alberta, T6G 2R3, Canada

Email: pdolez@ualberta.ca

Keywords: Fire-protective fabrics, high-performance fiber, hydrothermal aging, hydrolysis, mechanical Performance.

Abstract

Fire-protective fabrics made from high-performance fibers are available to provide protection from various hazardous conditions such as extreme heat and flame. However, these fabrics are often exposed to other deteriorating conditions, including moisture. It is a concern for the user's safety as some high-performance fibers are sensitive to hydrolysis. This study exposed eight fire-protective fabrics corresponding to typical blends used in firefighter protective suit outer shells to accelerated hydrothermal aging. They were immersed in water at different temperatures between 60°C and 95°C for up to 1200 hours. After exposure to hydrothermal aging, some fabrics exhibited a significant loss in tensile strength without any morphological changes. Based on results from energy-dispersive X-ray spectroscopy and pH measurements of the aging water, the larger loss in strength experienced by the para-aramid/PBI fiber-based fabrics can be related to the high amount of sulfur measured in the PBI fibers, contributing to an acceleration of the para-aramid fiber's hydrolysis in acidic conditions. Hydrothermal aging also appears to affect the water-repellent finish of some fabrics. The study provides an insight into the effect of a generally ignored hazard, i.e., moisture, on the long-term performance of fire-protective fabrics.

1. Introduction

Fire-protective fabrics are widely used for manufacturing protective clothing for first responders such as firefighters and defense personnel.[1] This type of fabric is also being used to produce workwear for oil and gas industry workers and electricians. The primary purpose of fire-protective clothing is to protect the wearer from heat and flame, providing enough insulation from the heat source to perform the tasks and/or move to safety.[2] Therefore, fire-protective fabrics should be flame resistant and not conduct heat. In addition, they should offer good mechanical performance to preserve the physical integrity of the clothing while in service.[3]

Two types of fibers are used in fire-protective fabrics[4]: fibers chemically modified with flame-retardant (FR) compounds and inherently fire-resistant fibers. Flammable textile fibers such as cotton, viscose, polyester, nylon, etc., can be modified by FR additives or finishes depending on the case to provide them with flame-resistant properties. However, the treated fibers are generally limited to a 100°C continuous operating temperature, above which they will start degrading.[5] Besides, FR finishes may get removed as a result of wear and laundering, for instance.[1] On the other hand, inherently flame-resistant fibers provide excellent protection against flame and extreme heat, and have a continuous operating temperature above 150°C.[5]

Several categories of inherently flame-resistant fibers are available such as aromatic polymeric fibers, carbon fibers, and inorganic fibers.[6] Among these, aromatic polymeric fibers are most widely used to manufacture fire-protective fabrics due to their low weight. [7] Para-aramid and meta-aramid fibers are part of the family of aromatic polyamides.[8] Their aromatic structure gives them excellent flame and heat resistance properties. For instance, para-aramid and meta-aramid fibers possess a continuous operating temperature of 190°C and 200°C, respectively.

Polybenzimidazole (PBI) and polybenzoxazole (PBO) are also inherently flame-resistant aromatic polymeric fibers, with a thermal index of 250°C and 310°C, respectively.[9] Other high-performance fibers such as liquid crystal polyester (LCP), polyamide-imide, novoloid, melamine, glass, and carbon fibers are also found in fire-protective fabric blends.[10]

Although these inherently flame-resistant fibers show excellent protective properties when new, their performance can diminish over time. In fact, a series of studies revealed that the mechanical and barrier performance of used firefighters' protective clothing was severely affected over time. [11–15] For instance, 65% of the four-year-old or less garments tested did not meet the water penetration requirement of the NFPA 1971 specification[16] of the National Fire Protection Association (NFPA), and 10% of them failed the mechanical performance requirements.[11] Surprisingly, some of these severely affected protective suits were still in use, which is a serious safety concern.

Accelerated aging campaigns have also been conducted on fire-protective fabrics. Arrieta et al. investigated the thermal aging behavior of yarns and fabrics composed of blends of para-aramid and PBI staple fibers and filaments.[17] They reported a loss in the mechanical performance of these materials due to extended exposure to high temperatures. A follow-up analysis by X-ray diffraction and Raman spectroscopy showed an increase in the crystallite size in the para-aramid fibers in the direction parallel to the coplanar sheets along with a disruption of the crystalline lattice in the perpendicular direction.[18] Furthermore, a study by Dolez et al. confirmed the negative impact of thermal aging on seven different fire-protective fabrics made of blends of para-aramid, meta-aramid, PBI, PBO, and melamine fibers.[19] They found a significant reduction in the tear strength of all seven fabrics over time, even when exposed to temperatures as low as 150°C.

Apart from thermal exposure, fire-protective fabrics also get exposed to ultraviolet (UV) radiation, abrasion, moisture, and laundering among others.[20] Houshyar et al. found a 79% drop in the mechanical performance of a para-aramid/PBI blended fire-protective fabric due to exposure to accelerated UV aging.[21] Arrieta et al. performed Attenuated Total Reflectance – Fourier Transform Infrared (ATR-FTIR) analysis on a UV aged para-aramid/PBI blended fabric.[22] The authors reported evidences of a photo-oxidative reaction leading to amide bond cleavage in the para-aramid fibers, which they thought caused the drop in the mechanical performance of the aged fabric.

In case of hydrothermal aging, firefighters' protective clothing gets exposed to water from weather and the fire-extinguishing medium.[20] Besides, the wearers' perspiration may also contribute to the fabric's moisture content.[23-24] Arrieta et al. showed the detrimental effect of hydrolytic aging conditions on a para-aramid/PBI blended fire-protective fabric.[22] They observed a 50% decrease in the residual tensile strength of yarns collected from the aged fabric specimens when exposed to 60% relative humidity (RH) at 80°C for 31 days. The sensitivity of para-aramid fibers to hydrolysis was mentioned as a possible reason for the degradation of the fabric's mechanical performance observed. During the processing of aramid fibers, microvoids are formed in the fiber.[25-26]; the resulting increase in surface area may increase the fiber's ability to absorb moisture. In addition, polymers that contain ester, ether, or amide groups are susceptible to hydrolysis and moisture-related degradation.[27] When this type of polymer comes into contact with moisture, chain scission occurs, which may cause the molecular weight of the polymer to decrease and reduce its mechanical properties. In a study, Engelbrecht-Wiggans et al. reported a 14% reduction in para-aramid yarns' tensile strength after aging at 76% RH and 70°C for one year.[28] However, they did

not observe any chemical changes in the aged fibers when measured with ATR-FTIR. Li et al. investigated the structure of para-aramid fibers after long-term exposure to different RH aging environments at temperatures between 60°C and 90°C.[29] They did not find any evidence of changes in the crystal structure of the aged fibers. Researchers have also found a negative impact of moisture aging on fabrics that contained PBO fibers. For instance, Chin et al. exposed twenty-four woven PBO body armor panels to RHs of 37% and 60% at 50°C and 60°C for up to 157 days.[30] Tensile strength tests performed on PBO yarns extracted from the aged fabrics revealed approximately 40% of strength reduction due to aging. Furthermore, FTIR analysis of aged specimens revealed the evidence of benzoxazole ring-opening in the PBO chemical structure followed by the formation of carboxylic acid and aminophenol groups, which was associated with the hydrolysis of PBO.

The care and maintenance procedure of fire-protective suits also involves water that may contribute to the degradation of the fire-protective fabrics. For instance, the NFPA 1851 standard specifies routine and advanced cleaning procedures of firefighters' protective ensembles.[31] The routine procedure includes brushing off debris and rinsing with water. A soft bristle brush with mild detergent and water is also recommended to remove stains or clean heavily soiled areas in the ensembles. At least twice a year or when the routine procedure is not sufficient to clean the suit, advance cleaning is performed by trained personnel using a washing machine with mild detergent and water at 40°C or below, followed by either air or machine drying. In a study, seven fabrics corresponding to different fiber blends used in fire-protective clothing were subjected to up to 50 washing and drying cycles as per NFPA 1971 washing/drying sample preparation procedure.[32] The authors reported a reduction of up to 66% in the tearing strength of the fabrics after 50 washing and drying cycles. This decrease in the fabrics' tear strength varied with their fiber content. They

observed a high reduction in the tear strength of most of the fabrics that contained a high percentage of para-aramid fibers. No significant changes were measured in meta-aramid-based fabrics. Makinen investigated some thermal, mechanical, and comfort properties of four fabrics - aramid, FR cotton, FR wool, and FR viscose blend - after subjecting them to up to 50 laundering cycles.[33] They reported an increase in the water absorption and a decrease in the air permeability of these four fabrics due to the repeated launderings. Nazare et al. subjected four fire-protective fabrics to five washing cycles followed by air drying.[34] The four fabrics had the same fiber content of 60% para-aramid / 40% melamine but different physical properties and surface chemical finishes. The authors reported a 20% reduction in the tear strength of one of the fabrics that did not have a surface finish, while the effect of the five washing cycles was minimal for the fabrics with a surface finish.

To further the knowledge about the effect of service conditions on the long-term performance of high-performance fibers, this study focuses on the exposure of fire-protective fabrics to accelerated hydrothermal aging conditions. The residual mechanical performance and surface condition of eight fire-protective fabrics were assessed after immersion in water at different temperatures and for different durations. The activation energy of the hydrothermally aged fabrics was extracted from the strength data to quantify the effect of temperature in hydrothermal aging. Chemical analysis was performed on the unaged fabrics to try identifying parameters contributing to the hydrothermal aging process.

2. Material and Methods

2.1. Materials

Eight fire-protective fabrics composed of different blends of para-aramid, meta-aramid, PBI, PBO, LCP, and anti-static carbon fibers were selected for this study. They are widely used as outer shell

fabrics in firefighters' protective clothing. **Table 1** provides the textile characteristics of these fabrics. According to their technical datasheets, they all comprise a water repellent finish. **Table 1** also lists the type(s) of yarn, fiber content, and linear density in the warp direction. Upon reception, the fabrics were kept in the dark at room temperature.

**Table 1:** Characteristics of the fabrics studied

Fabric Code/Group	Fabric Composition [a]	Fabric Structure [b]	Mass [b] (gram/m²)	Thickness [b] (mm)	Fabric Count [b] (yarn/cm) Warp	Weft	Warp yarn Fiber content [b]	Yarn type [b]	Linear density [c] (tex)
MA Group 1	64% para-aramid & 36% PBI	Twill weave	234	0.50	18	17	PBI & para-aramid	Spun	93
							Para-aramid	Spun + Filament	68
MB Group 1	55% para-aramid, 37% PBI & 8% LCP	Plain weave	246	0.48	16	15	PBI & para-aramid	Spun	100
							Para-aramid & LCP	Spun + Filament	78
MC Group 2	65% para-aramid & 35% meta-aramid	Broken twill weave	222	0.40	24	24	Meta-aramid & para-aramid	Spun	56
							Para-aramid	Filament	48
MD Group 2	60% para-aramid & 40% meta-aramid	Twill weave	227	0.48	18	18	Meta-aramid & para-aramid	Spun	109
							Para-aramid	Spun	59
ME Group 2	60% para-aramid, 20% meta-aramid & 20% PBO	Twill weave	226	0.50	19	18	Para-aramid, meta-aramid & PBO	Spun	62
								Spun	59
MF Group 2	93% meta-aramid, 5% para-aramid & 2% Anti-Stat	Plain weave	257	0.60	28	17	Meta-aramid & para-aramid	Spun	51
MG Group 1	65% para-aramid & 35% PBI	Twill weave	214	0.38	24	22	PBI & para-aramid	Spun	53
							Para-aramid	Filament	46
MH Group 1	65% para-aramid & 35% PBI	Twill weave	247	0.43	19	20	PBI & para-aramid	Spun	79
							Para-aramid	Filament	66

[a] From the manufacturer, [b] From [35], [c] From [36]

2.2. Accelerated Aging

Accelerated hydrothermal aging was conducted by fully immersing fabric specimens into reverse-osmosis (RO) water at different temperatures for up to 50 days (1200 hours). Four of the fabrics were exposed to hydrothermal aging at 60, 80, and 90°C. For the four other fabrics, the temperature of 95°C was added to the experiment program since the changes in mechanical performance recorded between 60 and 90°C were limited. Specimens of 15 x 2.5 cm were wetted in a RO water tray using a 1 kg roller (**Figure 1**). Then, the wetted specimens were placed in flasks containing RO water at the selected temperature. The flasks were kept in a convection oven (Heratherm™, ThermoFisher Scientific, Ottawa, ON, Canada) for the specified durations. RO water at the same temperature as the oven was added at regular intervals in the flasks to compensate for evaporation. Aged specimens were collected every five days for the total period of 50 days. They were kept flat to dry at room temperature.

Using the same convection oven, the fabric specimens were exposed to thermal aging at 90°C in the air for three exposure times (15, 30, and 50 days). The specimens were attached with clips to the oven shelf so that they hung vertically with a distance of about 2 cm between them. The five replicates for each condition were distributed in the oven. Tests were also run in RO water at 21°C with an exposure time of 50 days.
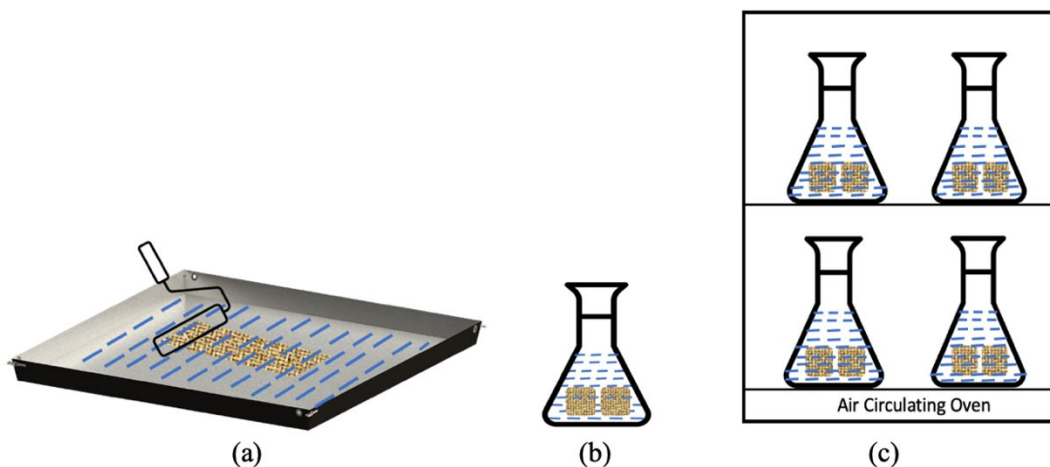
Figure 1: Schematic representation of the hydrothermal aging protocol -a) specimen wetting procedure, b) specimens immersed into RO water at the selected temperature, c) flasks kept in an air-circulating oven.

2.3. Residual Tensile Strength

The effect of hydrothermal aging on the fabrics' mechanical performance was monitored by characterizing the specimen's residual ultimate tensile strength. The force at break of unaged and hydrothermally aged fabric specimens was measured in the warp direction following the ASTM D5035 (strip test) test standard.[37] According to this test method, 15 x 3.5 cm strip specimens are ravelled to 2.5 cm by removing yarns from both long sides of the specimens. For each type of fabric, the number of yarns in the ravelled specimens was kept constant to ensure a good reproducibility of the strength results (Table S1, Supporting Information). The hydrothermal and thermal aging described in the previous section was conducted on the ravelled specimens.

The specimens' force at break was measured with a mechanical test frame (Instron 5565, Illinois Tool Works Inc., Norwood, MA) equipped with a 5kN load cell and pneumatic (517 kPa) clamps with rubber faces. The specimens were tested until failure at a 100 mm/min rate with a gauge

length of 75 mm. The tests were performed on specimens that had been conditioned at a temperature of 20 ± 2°C and a RH of 65 ± 2% according to CAN/CGSB-4.2 No-M88[38] for at least 24 hours after having dried up.

The time-temperature superposition (TTS) principle was used to analyze the effect of the hydrothermal aging on the fabric strength. The TTS principle is widely accepted in polymer science either to determine the temperature dependency of viscoelastic polymers or to interpolate the time or frequency at a specific temperature at which the material's behavior has been investigated.[39] The use of the TTS principle improves the accuracy of the extraction of polymers' activation energy and lifetime prediction.[40] According to the TTS theory, the material's properties obtained after short-term exposure to a higher temperature are equivalent to its property obtained by exposing the material to a lower temperature for a prolonged time.[19] Accordingly, a master curve was constructed by shifting horizontally the data corresponding to the different aging temperatures displayed on a semi-logarithmic plot onto the data corresponding to a reference aging temperature.

Then, the Arrhenius model was used to analyze the effect of the aging temperature on the fabric strength: the logarithm of the shift factors was plotted as a function of the reciprocal aging temperature. This model assumes that the degradation of the material is homogenous, with one chemical reaction describing the whole process.[19] In the Arrhenius equation (Equation 1), K denotes the material's degradation reaction rate, E_a represents the activation energy, which illustrates the sensitivity of the material to the thermal aging conditions, and R and T correspond to the universal gas constant and the absolute temperature, respectively.

$$K = K_0 \exp(\frac{-E_a}{RT})$$ (1)

2.4. Optical Microscopy

A stereo optical microscopy (Zeiss Stemi 508, Germany) was used for the surface morphology analysis of unaged and hydrothermally aged fabric specimens. Images were captured in reflected light mode.

2.5. Scanning Electron Microscopy

The surface morphology of unaged and hydrothermally aged fabric specimens was analyzed by Scanning Electron Microscopy (SEM) (Zeiss EVO 10, Germany). Prior to imaging, the specimens were gold-coated by sputtering (Denton sputter gold coating machine) with a thickness of 16 nm. The acceleration voltage was 10 kV. The SEM analysis of the specimens was performed at different magnifications to cover the features from fabric scale to individual fiber.

2.6. Energy Dispersive X-ray Spectroscopy

An energy-dispersive X-ray spectroscopy (EDX) machine (Zeiss EVO 10, Germany) and the Aztec software were used to perform the elementary analysis of the unaged fabrics. The acceleration voltage was 20 kV, and the working distance was 8.5 mm. The analysis was performed on the fabric surface, bundles of fibers, and yarn cross-section.

2.7. Water Contact Angle

The water contact angle measurement was performed on unaged and hydrothermally aged fabric specimens using the sessile drop technique (FTA-200, First Ten Angstroms Inc., Newark, CA). A

0.3 µL volume of RO water was dropped on the surface of the fabric specimen (**Figure 2-a**). Images of the water drop on the fabric surface were taken every 0.2 seconds. The contact angle between the surface of the specimen and the water droplet was determined by image analysis using the first recorded image after the water deposition on the fabric surface (**Figure 2-b**). For each specimen, the water contact angle measurement was performed at 25 different locations covering both faces of the specimen.

(a)   (b)
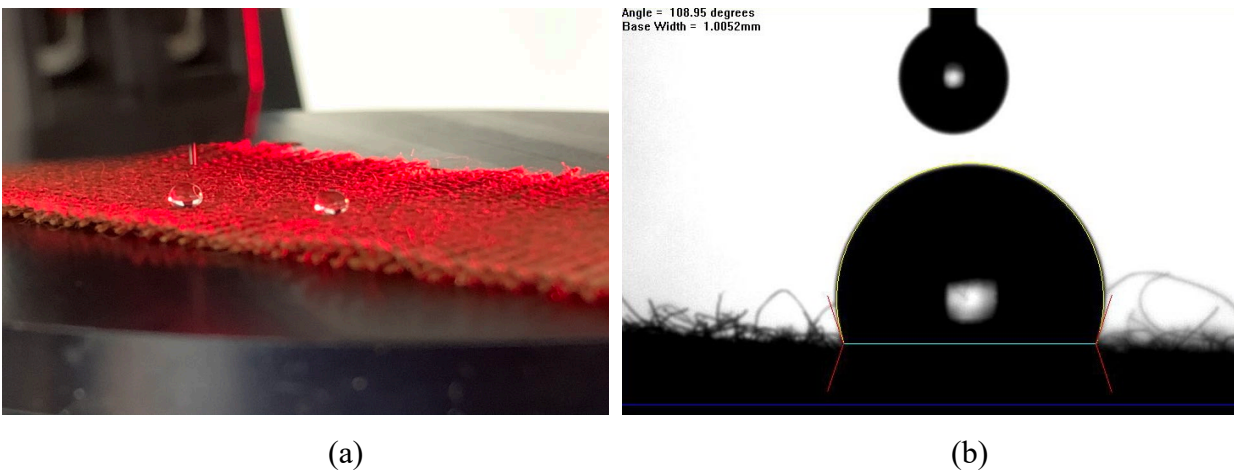
Figure 2: Water contact angle measurement- a) RO water droplet on the fabric specimen, b) Measurement of the water contact angle by the image analysis software.

2.8. Liquid Absorbency Capacity

The liquid absorptive capacity (LAC) measurement of unaged and hydrothermally aged specimens was performed according to the ISO 9073-6 standard test method[41] with a slight modification in terms of the size of the specimens, which was 13.5×2 cm. First, specimens were immersed in RO water for 60 seconds, and then held vertically for 120 seconds to drain excess liquid. Finally, water droplets remaining on the surface of the specimens were removed by applying a 16.5 g/cm^2 pressure to the fabric specimen sandwiched between two layers of paper towel. The weight of the

fabric specimens was measured using a Mettler Toledo PJ3000 balance (Mettler-Toledo, New Zealand, capacity 3100g, readability 0.01g).

2.9. pH Measurement

A digital pH meter (SevenCompact pH meter S220, Mettler Toledo, Canada) was used to measure the pH of the RO water in the flasks where the fabrics had been hydrothermally aged.

2.10. Statistical Analysis

T-tests were performed on the data when relevant. A p-value of 0.05 was considered, whereas a p-value greater than 0.05 denotes no significant differences between the data of two groups of specimens.

3. RESULTS

3.1. Mechanical Performance

The residual tensile strength of the hydrothermally and thermally aged fabrics was measured and compared with the tensile strength of the unaged fabrics. For the presentation of the results, the fabrics studied have been grouped based on their fiber content. Group 1 fabrics are mainly based on a blend of para-aramid and PBI fibers, whereas Group 2 fabrics contain meta-aramid fibers in blend with para-aramid and PBO fibers. Each group contains four fabrics.

3.1.1. Group 1: Para-aramid/PBI-based fabrics

Group 1 includes Fabric MA, MB, MG, and MH. Among these four fabrics, MA, MG, and MH fabrics contain only para-aramid and PBI fibers. On the other hand, Fabric MB contains 8% of LCP fibers along with the para-aramid and PBI fibers. The hydrothermal aging behavior of these

four fabrics is shown in **Figure 3**. For each fabric, the results are displayed in terms of breaking force retention as a function of aging time for three hydrothermal aging temperatures (60, 80, and 90°C) and one thermal aging temperature (90°C).

As shown in **Figure 3**, all four fabrics experienced a gradual decrease in tensile strength with the increase in hydrothermal aging time and temperature. After 50 days of hydrothermal aging at 90°C, Fabric MA experienced the largest loss in tensile strength (75%) among these four fabrics, while MH experienced the lowest loss (57%). Although Fabric MA and MH contain almost the same ratio of para-aramid and PBI fibers (64% para-aramid for MA and 65% para-aramid for MH) and have the same weave structure (Table 1), these two fabrics exhibit a statistically significant difference (p=0.0011) in their breaking force retention after 50 days of hydrothermal aging at 90°C. This may be due to the fact that they are from two different manufacturers, and thus may have experienced slight variations in the manufacturing process at the yarn and fabric level. They probably also have different water repellent finishes.

Furthermore, there is a significant difference (p=0.0012) in the strength retention between Fabric MG and MH. Fabric MG experienced a 68% loss in breaking force after aging at 90°C for 50 days, while Fabric MH displayed a loss of 57%. Although both fabrics have identical fiber content, weave structure, and are from the same manufacturer, they have a different weight per unit area. The weight of Fabric MG is 214 g/m^2, whereas Fabric MH's weight is 247 g/m^2. It is possible that the higher thickness of Fabric MH slowed down the degradation as it may take more time for water to reach fibers in the middle of the fabric thickness.
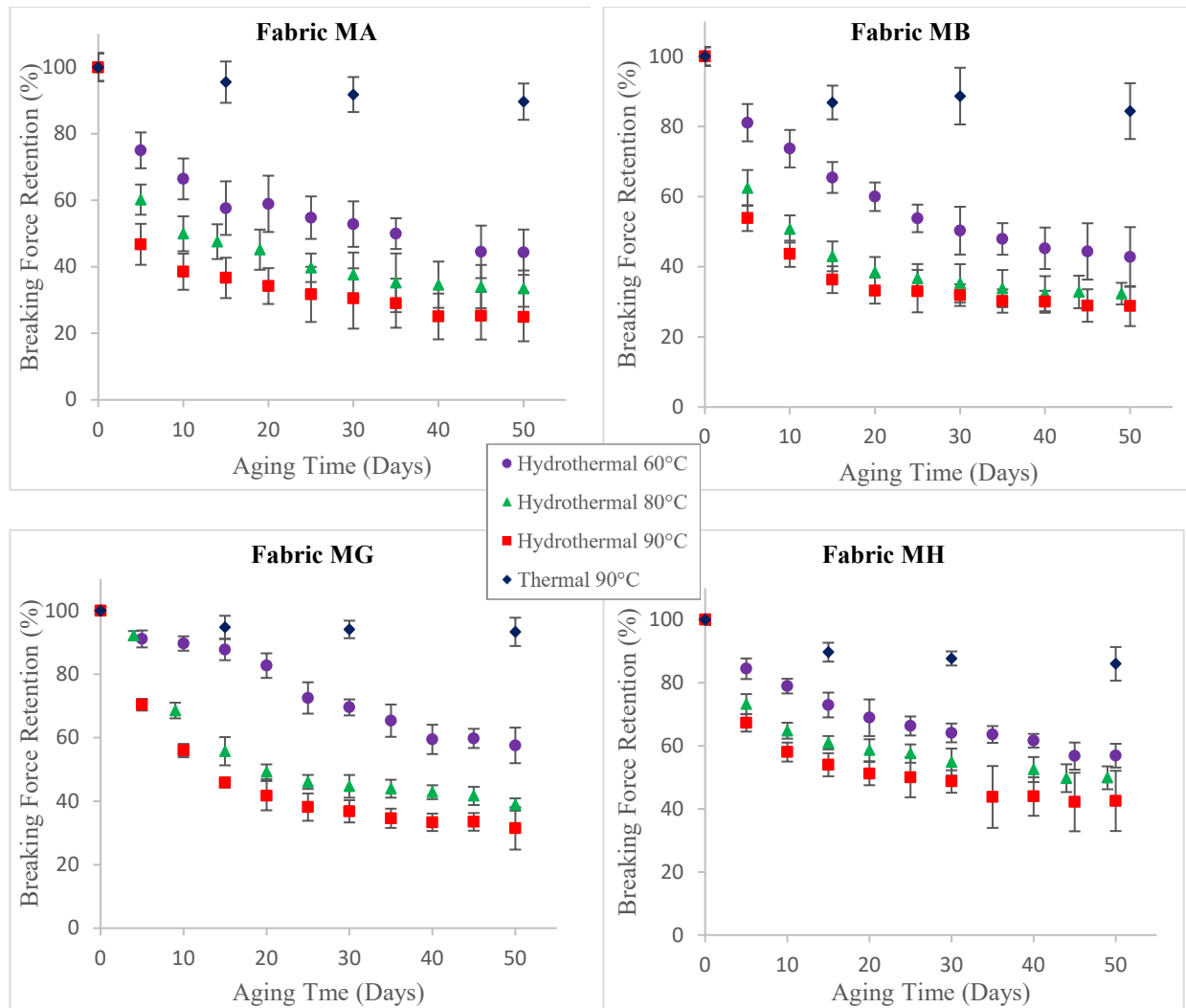
Figure 3: Residual breaking force of Fabric MA, MB, MG and MH as a function of aging time for hydrothermal aging temperatures of 60, 80 and 90°C and a thermal aging temperature of 90°C.

In addition, all the fabrics in Group 1 exhibited a significant loss in the force at break after 50 days of thermal aging at 90°C (p = 0.038 for MA, p = 0.029 for MB, p = 0.023 for MG and p = 0.016 for MH). Fabric MB lost 15% of its force at break, which was recorded as the highest loss among four fabrics, while Fabric MG lost its 7% force at break, which was recorded as the lowest loss among the four fabrics of Group 1. Fabric MA and MH experienced a 10% and 14% loss in force at break, respectively, due to the thermal aging at 90°C for 50 days. This loss in the mechanical

performance of all four fabrics comprising para-aramid and PBI fibers at a low temperature like 90°C is alarming as the continuous operating temperature reported for para-aramid and PBI fibers is 190°C and 250°C, respectively.[8-9]

The variation of the fabrics' breaking force retention has also been analyzed as a function of the hydrothermal aging temperature (60, 80 and 90°C). **Figure 4** shows the results for the different fabrics of Group 1 after 50 days of aging. The result at room temperature is also included. Three of the four fabrics exhibited a slight decrease in strength (p=0.063 for MA, p=0.043 for MB, and p=0.000 for MH) after 50 days of water immersion at 21°C: the loss in the force at break was 7%, 10%, and 10% for Fabric MA, MB, and MH, respectively. On the other hand, no statistically significant effect was measured for Fabric MG (p=0.228). For higher hydrothermal aging temperatures, all four fabrics in Group 1 exhibited severe degradation, with the breaking force retention showing a monotonous decrease as the aging temperature increased. These results confirm the large contribution of temperature to the loss in mechanical performance associated with the hydrothermal aging of para-aramid/PBI blended fire-protective fabrics, as already reported in the literature.[22]

It is interesting to note the difference in behavior between Fabric MG and MH, which have the same fiber content, weave structure, and are from the same manufacturer, but have a different weight per unit area. Fabric MG, which is the lightest, did not exhibit any statistically significant change in tensile strength after 50 days of water immersion at 21°C, while Fabric MH lost 10% when exposed to the same conditions. On the other hand, Fabric MG only had 31% breaking force

retention after 50 days of hydrothermal aging at 90°C, while Fabric MH still retained more than 42% of its strength.
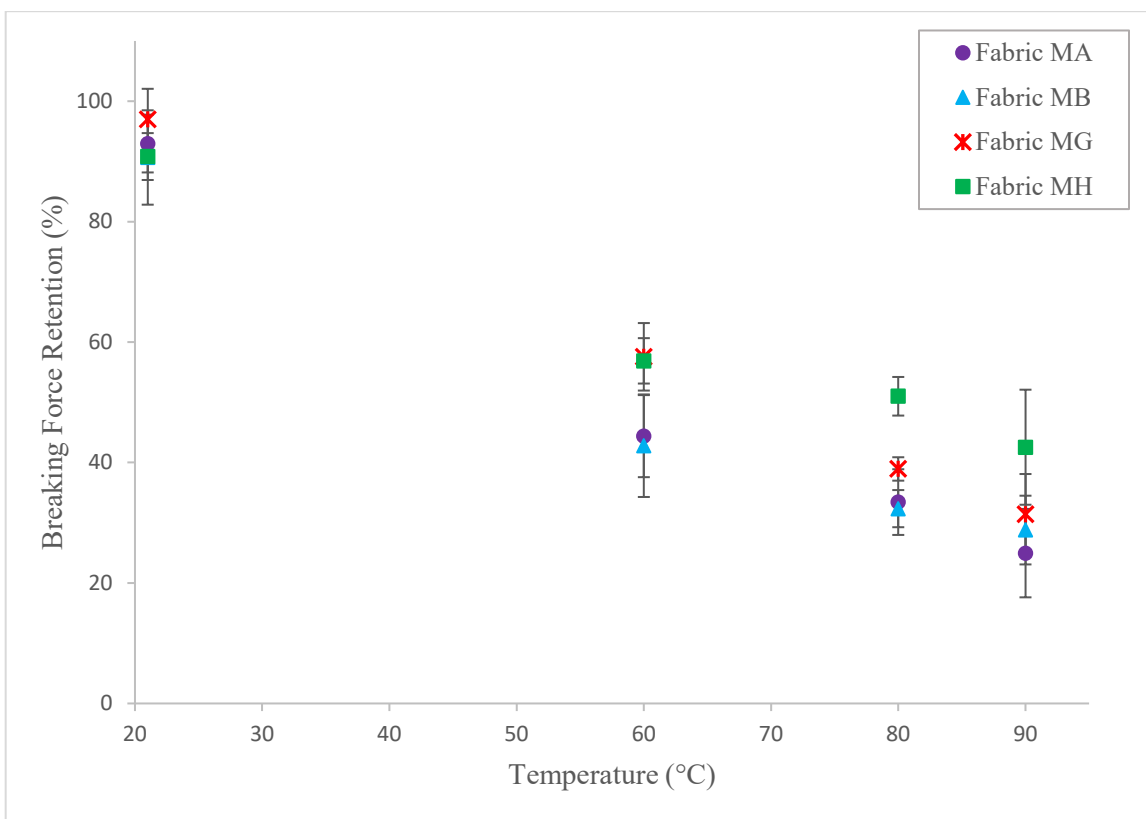
Figure 4: Residual breaking force retention for Fabric MA, MB, MG and MH as a function of the hydrothermal aging temperature for an aging time of 50 days.

The degradation behavior observed here for the para-aramid-based fabrics may be related to the sensitivity of para-aramid fibers to hydrolysis.[22,32,42] Hydrolysis leads to chain scission of the amide linkage in the aramid fiber in the presence of an acid or a base working as a catalyst. Arrieta et al. identified sulfur in their fabric, which they thought could have been a residue of the para-aramid spinning process and may have catalyzed the para-aramid hydrolysis.[22] They also proposed an acid-catalyzed hydrolysis mechanism of para-aramid fibers, shown in **Figure 5**. In addition, para-aramid fibers have a unique core skin structure, increasing the possibility of a

localized degradation of the core.[43] For its part, PBI fiber is not expected to be affected by water aging as it possesses an entirely aromatic structure.[22]
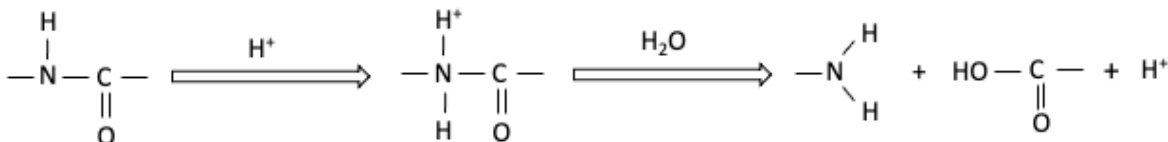
Figure 5: Acid catalyzed hydrolysis mechanism of para-aramid fiber.[22]

The TTS principle was combined with the Arrhenius model to quantify the contribution of temperature to the hydrothermal aging and its effect on the strength of the Group 1 fabrics. For this purpose, master curves (**Figure 6**) were constructed for each fabric using the residual tensile strength data for the specimens exposed to accelerated hydrothermal aging at 60°C, 80°C, and 90°C. To construct the TTS master curves, 60°C was used as the reference temperature. The shift factors provided by the TTS principle are displayed in an Arrhenius plot included as an insert in **Figure 6**. A linear relationship between the logarithm of the shift factors and the inverse of the absolute temperature was observed for all four fabrics of Group 1. This indicates that the contribution of temperature to the effect of hydrothermal aging on the tensile strength of the para-aramid/PBI-based fabrics can be described by the Arrhenius model within the range of the temperatures studied.
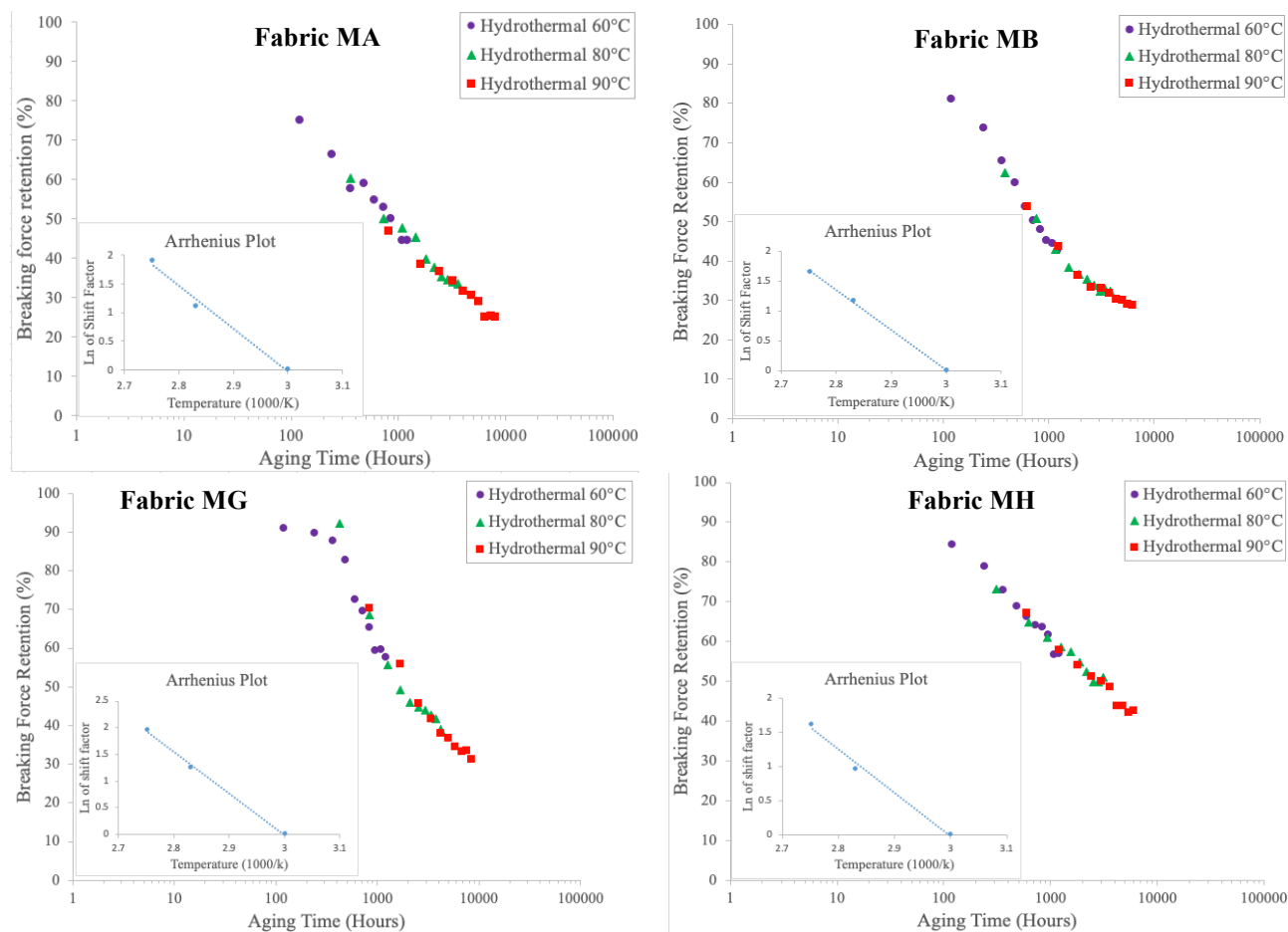
Figure 6: TTS master curve at 60°C for Fabric MA, MB, MG and MH (in insert: Arrhenius plot of the shift factors).

The activation energy corresponding to the contribution of temperature to the effect of hydrothermal aging on the fabric tensile strength was extracted from the Arrhenius plot for each fabric. The values are 62.2 ± 0.2 kJ mol^{-1} for Fabric MA, 55.54 ± 0.03 kJ mol^{-1} for Fabric MB, 64.60 ± 0.07 kJ mol^{-1} for Fabric MG, and 52.8 ± 0.1 kJ mol^{-1} for Fabric MH. By comparison, the activation energies reported by Dolez et al. for seven fire-protective fabrics with similar fiber contents that were exposed to thermal aging and assessed by tearing ranged between 95 and 113 kJ mol^{-1}.[19] The lower values obtained here for the contribution of temperature to the effect of hydrothermal aging on the fabrics' mechanical performance confirm the synergetic effect between

water and temperature on the aging of these para-aramid/PBI-based fire-protective fabrics, with the presence of water accelerating the aging associated with the thermal exposure.

3.1.2. Group 2: Meta-aramid-based fabrics

Group 2 includes Fabric MC, MD, ME, and MF. These four fabrics do not contain PBI fibers. Two of them, Fabric MC and MD contain only para-aramid and meta-aramid fibers. Fabric ME contains para-aramid, meta-aramid, and PBO fibers, while Fabric MF contains para-aramid, meta-aramid, and anti-static fibers. The meta-aramid fiber content in Group 2 fabrics ranges between 20% and 93%. The hydrothermal aging behavior of these four fabrics is shown in **Figure 7**. For each fabric, the results are displayed in terms of breaking force retention as a function of aging time for four hydrothermal aging temperatures (60, 80, 90, 95°C) and a thermal aging temperature (90°C).

As shown in **Figure 7**, fabrics in Group 2 did not exhibit a large loss in mechanical performance with hydrothermal aging. For instance, Fabric MC and MF experienced only a 12% and 4% decrease in their force at break, respectively, after 50 days of hydrothermal aging at 95°C. Fabric MD and ME showed some significant decrease in strength as a result of hydrothermal aging but only for aging temperatures of 80°C and above for Fabric MD and for aging temperatures of 90°C and above for Fabric ME. The reduction in breaking force was 47% after 50 days of hydrothermal aging at 95°C for Fabric MD and 25% for Fabric ME. Since there was little to no degradation for Group 2 fabrics after hydrothermal aging, the data analysis using the TTS principle and Arrhenius model could not be conducted.
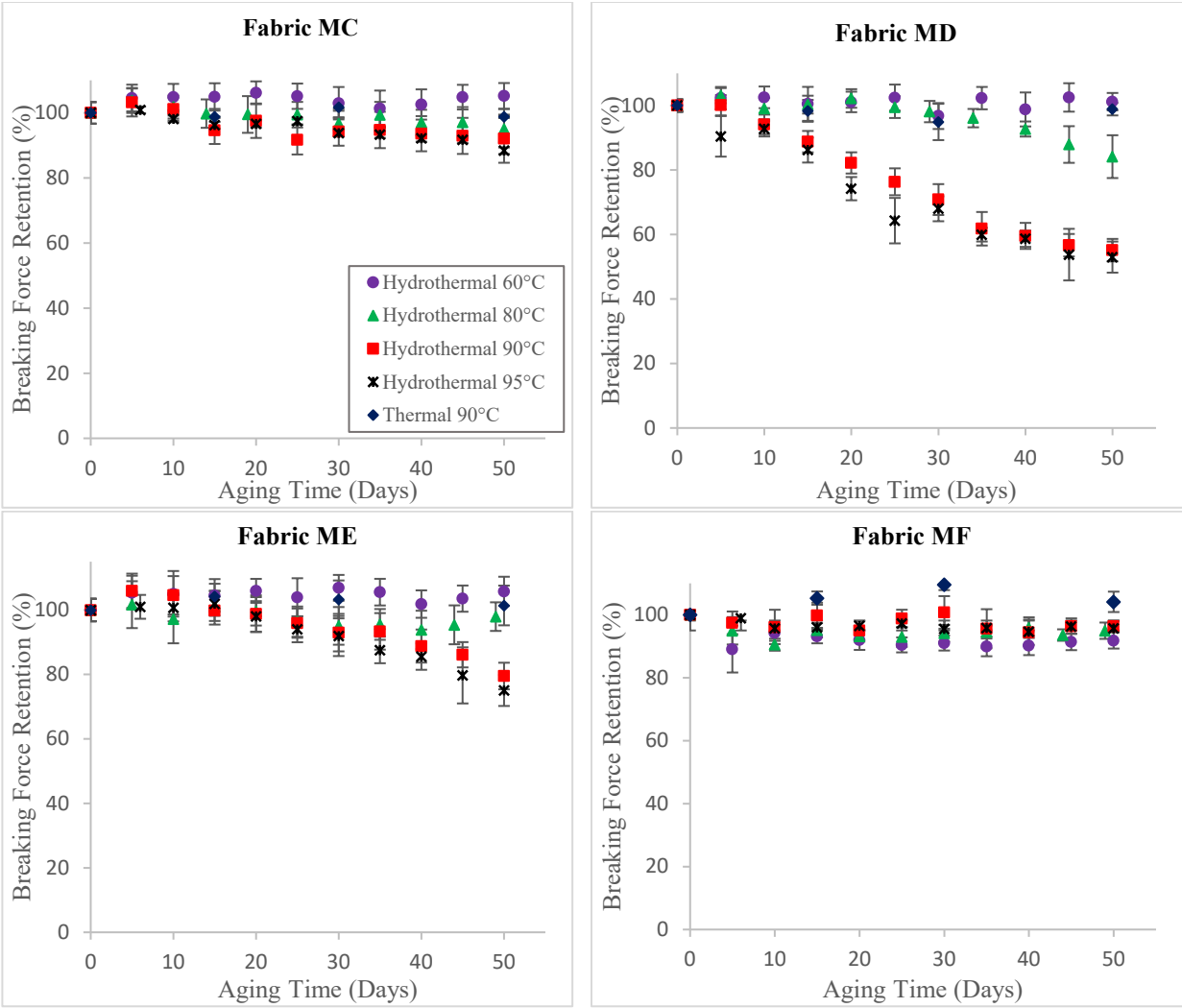
Figure 7: Residual breaking force of Fabric MC, MD, ME and MF as a function of aging time for hydrothermal aging temperatures of 60, 80, 90 and 95°C and a thermal aging temperature of 90°C.

In addition, none of the Group 2 fabrics experienced any significant loss in the force at break after 50 days of thermal aging at 90°C (p = 0.430 for MC, p = 0.670 for MD, p = 0.143 for ME, p = 0.107 for MF). This shows that thermal aging only at 90°C for up to 50 days does not impact the tensile strength of Group 2 fabrics.

The variation in the fabrics' breaking force retention as a function of the hydrothermal aging temperature (60, 80, 90, 95°C) is shown in **Figure 8**. The results for water immersion at room temperature are also included. Fabric MC did not exhibit any statistically significant change in strength after 50 days of water immersion at 21, 60, 80, and 90°C. Only after 50 days of aging at 95°C was a significant difference in strength recorded compared to the unaged value (p=.01): the fabric lost 12% of its force at break. The strength of the three other fabrics showed significant differences (p = 0.000 for MD; p = 0.024 for ME; p=0.005 for MF) after 50 days of water immersion at 21°C. The breaking force of Fabric MD and ME increased by 9% and 7%, respectively, whereas Fabric MF exhibited a 6% reduction in its breaking force. Fabric MD and ME showed a progressive decrease in force at break at 50 days for increasing aging temperatures. On the other hand, the strength of break of Fabric MF remained unaffected with the increasing hydrothermal aging temperature.
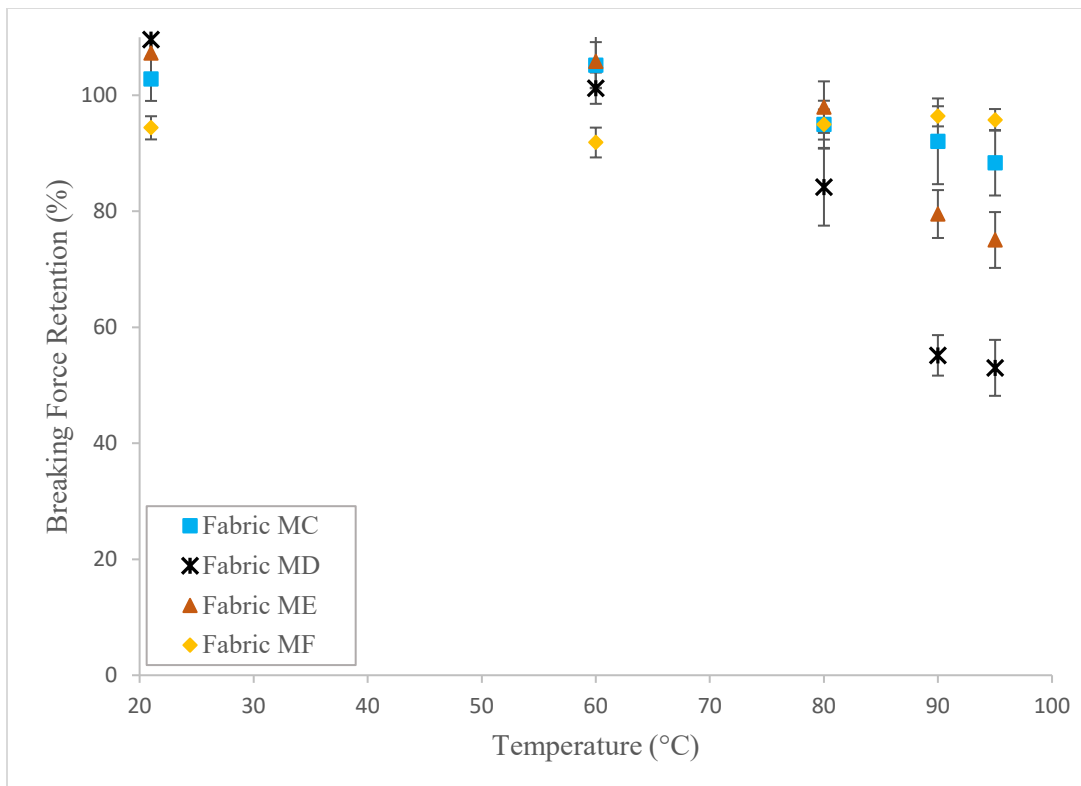
Figure 8: Residual breaking force retention for Fabric MC, MD, ME and MF as a function of the hydrothermal aging temperature for an aging time of 50 days.

The lower sensitivity to hydrothermal aging of Group 2 fabrics compared to Group 1 fabrics may potentially be associated with the fact that meta-aramid fibers are less affected by water than para-aramid fibers.[32] One reason may be the flexible structure of the meta-aramid molecule that allows a closer packing and prevents the easy penetration of water into the polymer structure.[43] Furthermore, unlike para-aramid fibers, meta-aramid fibers are not prone to localized core structure degradation due to a similar structure for the core and the skin.[21]

3.2. Chemical Analysis

EDX analysis has been performed on all eight fabrics in the unaged condition to look for the presence of sulfur in the fabrics, which was identified by Arrieta et al. in their para-aramid/PBI fabric and linked to its sensitivity to hydrothermal aging.[22] **Figure 9** shows a representative EDX layered image for each of the eight fabrics studied, as well as the corresponding EDX spectra showing the different elements identified.
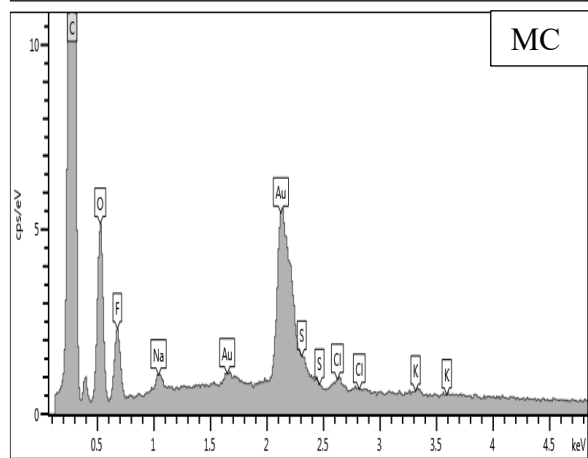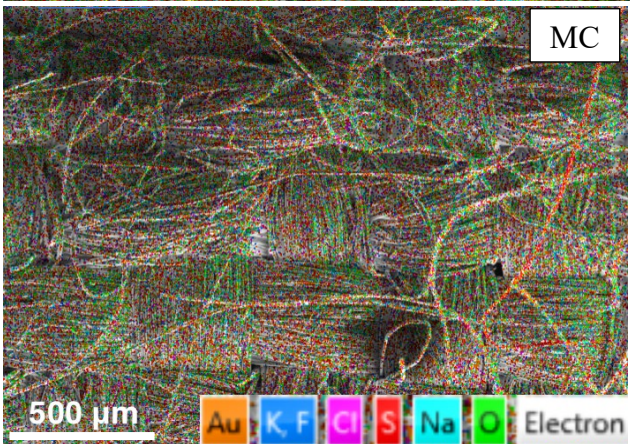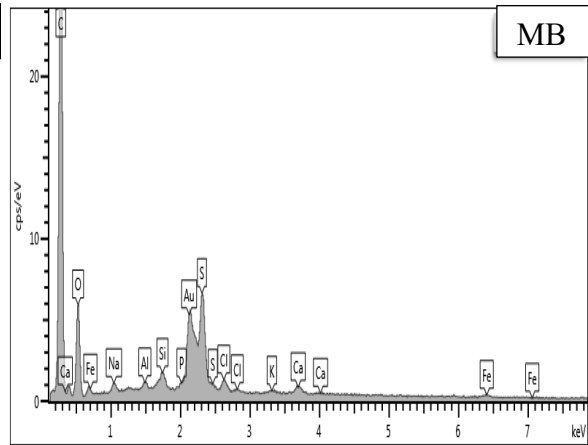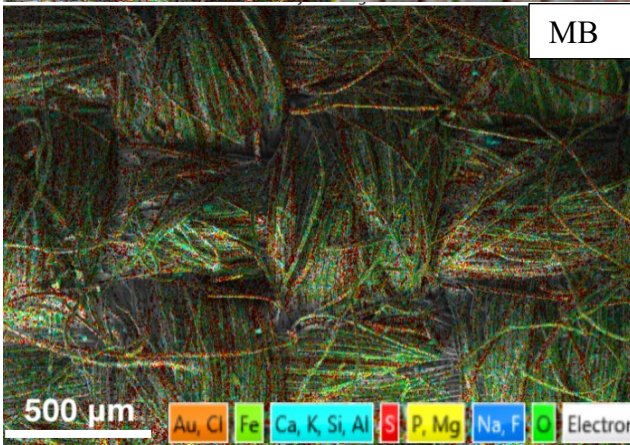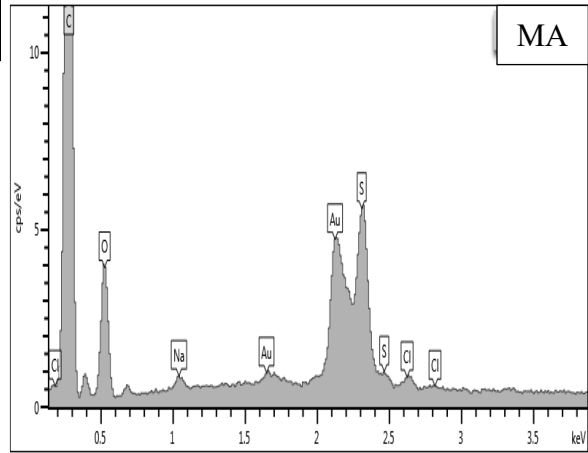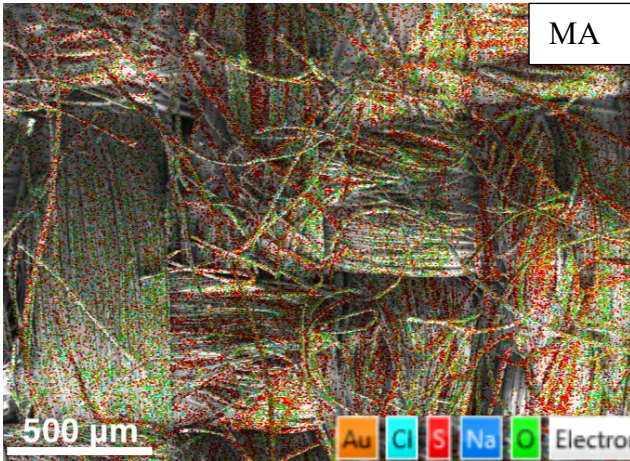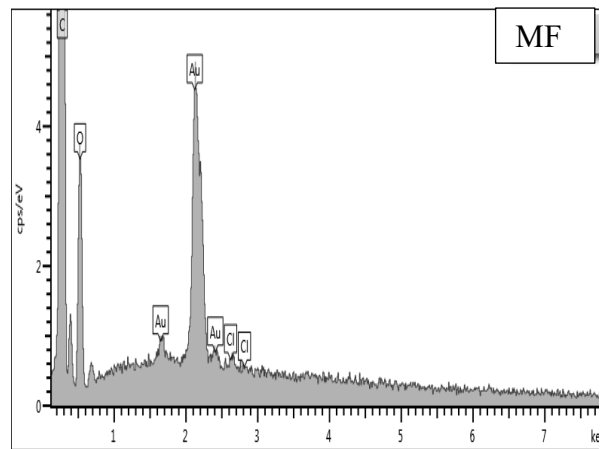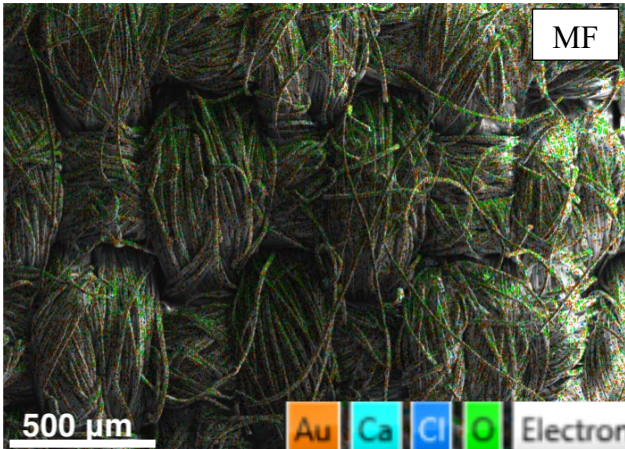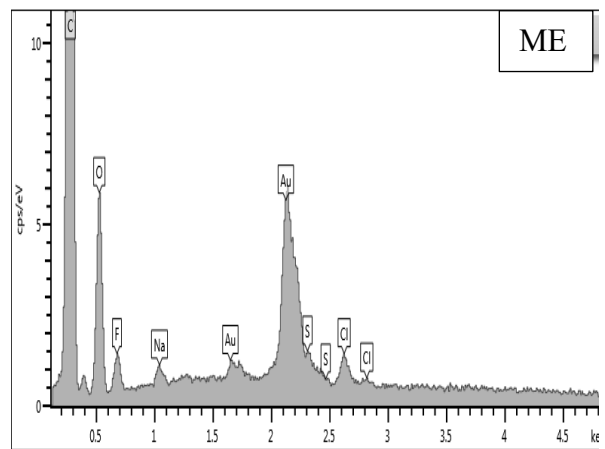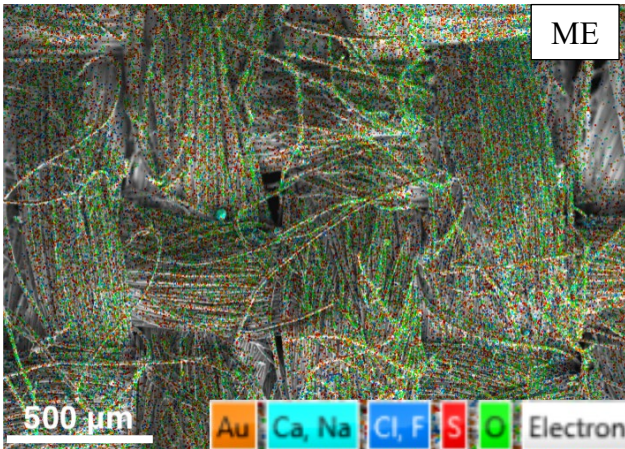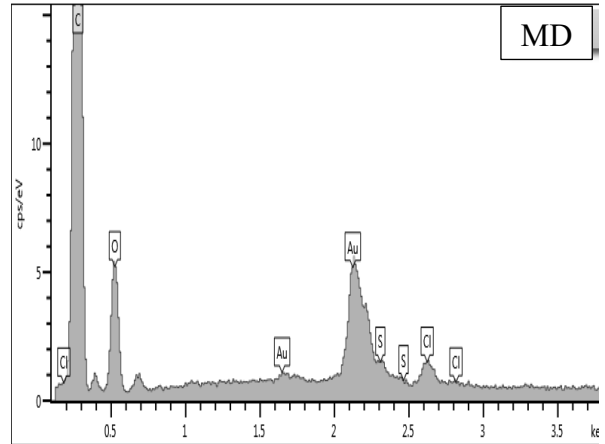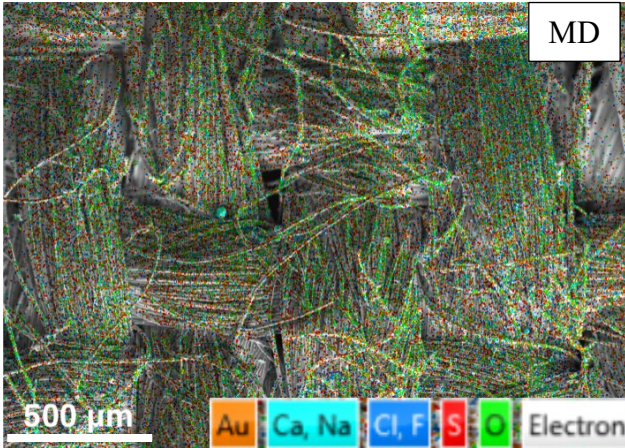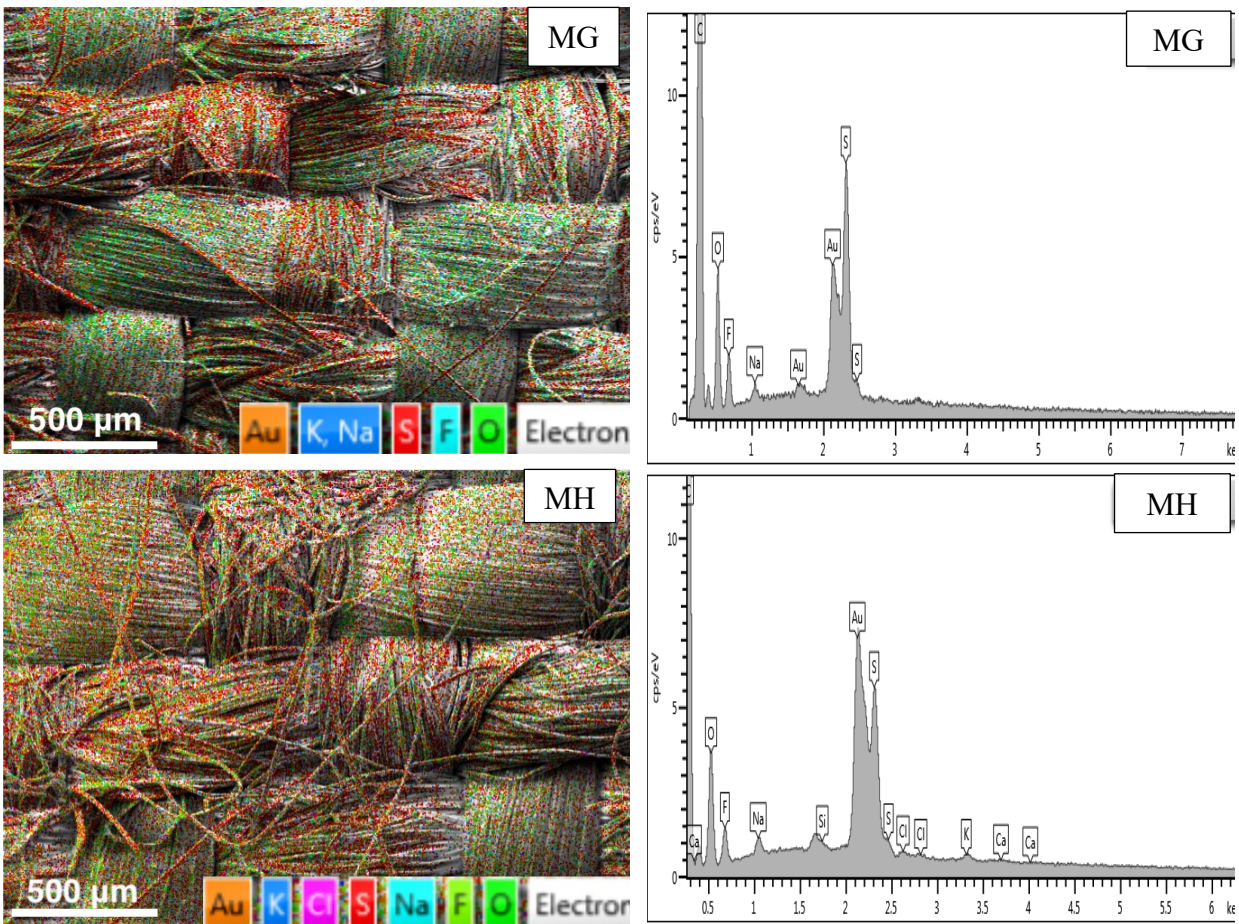
Figure 9: Example of EDX layered image and spectrum for each fabric (sulfur appears in red in the EDX images).

In the case of Group 1 fabrics (Fabric MA, MB, MG, MH), the presence of sulfur in a large proportion can be observed. Sulfuric acid is used in the yarn spinning process of both para-aramid and PBI fibers[44]; this could explain the presence of the sulfur observed in para-aramid/PBI-containing fabrics. EDX analyses were performed on specific areas corresponding to the spun yarns and filament yarns for Fabric MG and MH (in the unaged condition). **Table 2** provides the sulfur content for a series of analysis on para-aramid/PBI spun yarns and para-aramid filament yarns in Fabric MH. The sulfur content in areas corresponding to para-aramid filament yarns is 0.37 ± 0.05%, while the sulfur content in areas corresponding to para-aramid/PBI spun yarns is

$1.3 \pm 0.2\%$. The difference in sulfur content between the para-aramid filament yarns and para-aramid/PBI spun yarns is statistically significant ($p = 0.000$). Similar results were obtained for Fabric MG. This may indicate that PBI fibers contain more sulfur than para-aramid fibers/filaments.

By comparison, the amount of sulfur in Group 2 meta-aramid-based fabrics (**Figure 9**) is much lower. For instance, Fabric MF did not exhibit any traces of sulfur. Fabric MC, MD, and ME barely showed any traces of sulfur. An analysis of specific areas corresponding to para-aramid/meta-aramid spun yarns and para-aramid filament yarns were performed for Fabric MC. The results are shown in **Table 3**. The average values of sulfur content are between 0.23 and 0.29. This is comparable to the value recorded for the para-aramid filament yarns in Fabric MG and MH but much lower than the value measured for the para-aramid/PBI spun yarns.
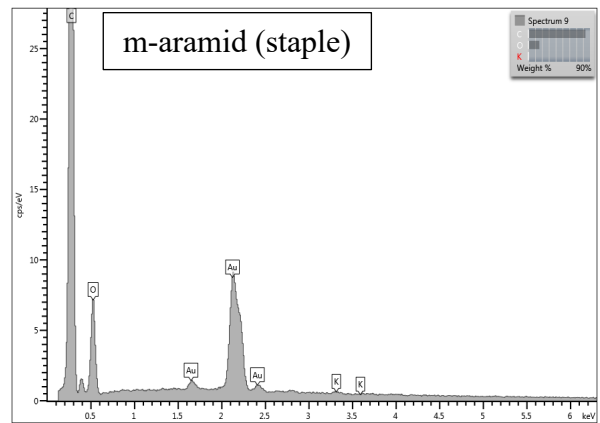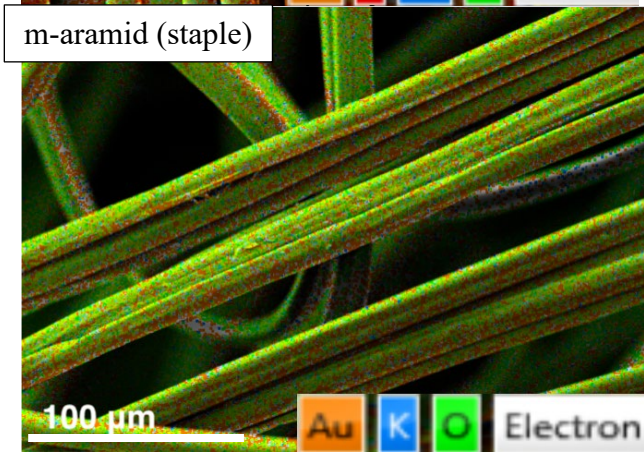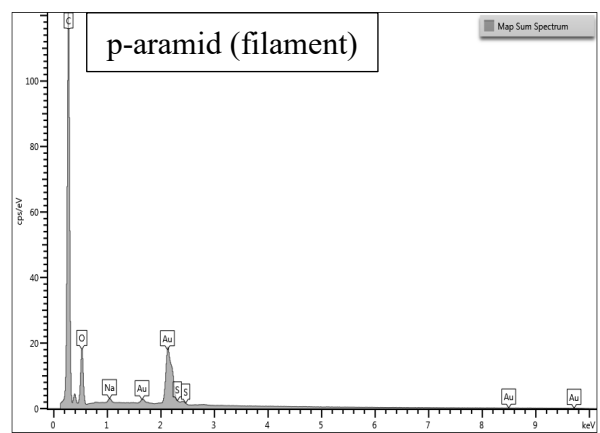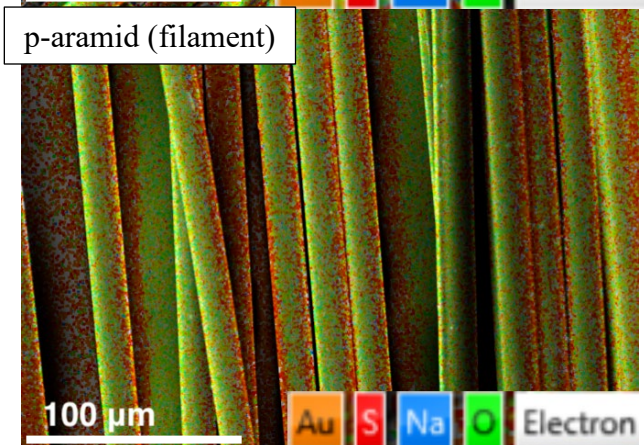
Table 2: Sulfur content in specific areas corresponding to the spun yarns and filament yarns for Fabric MH in the unaged condition (areas circled in red correspond to para-aramid filament yarns and areas in green to para-aramid/PBI spun yarns).

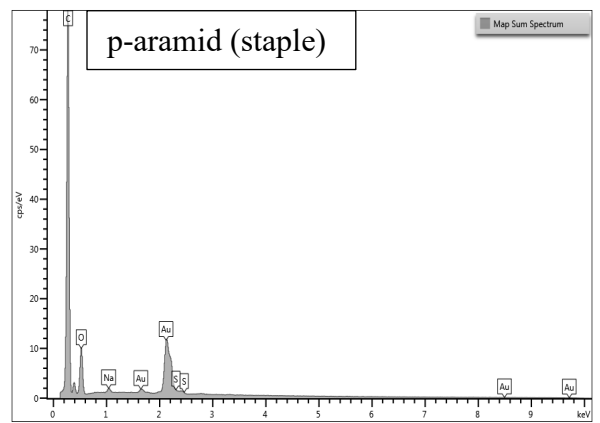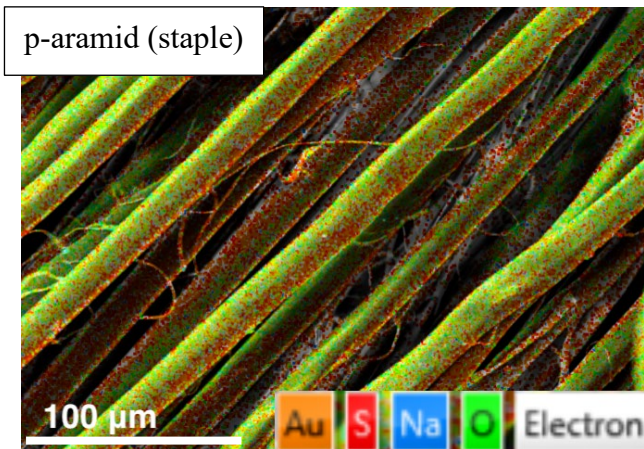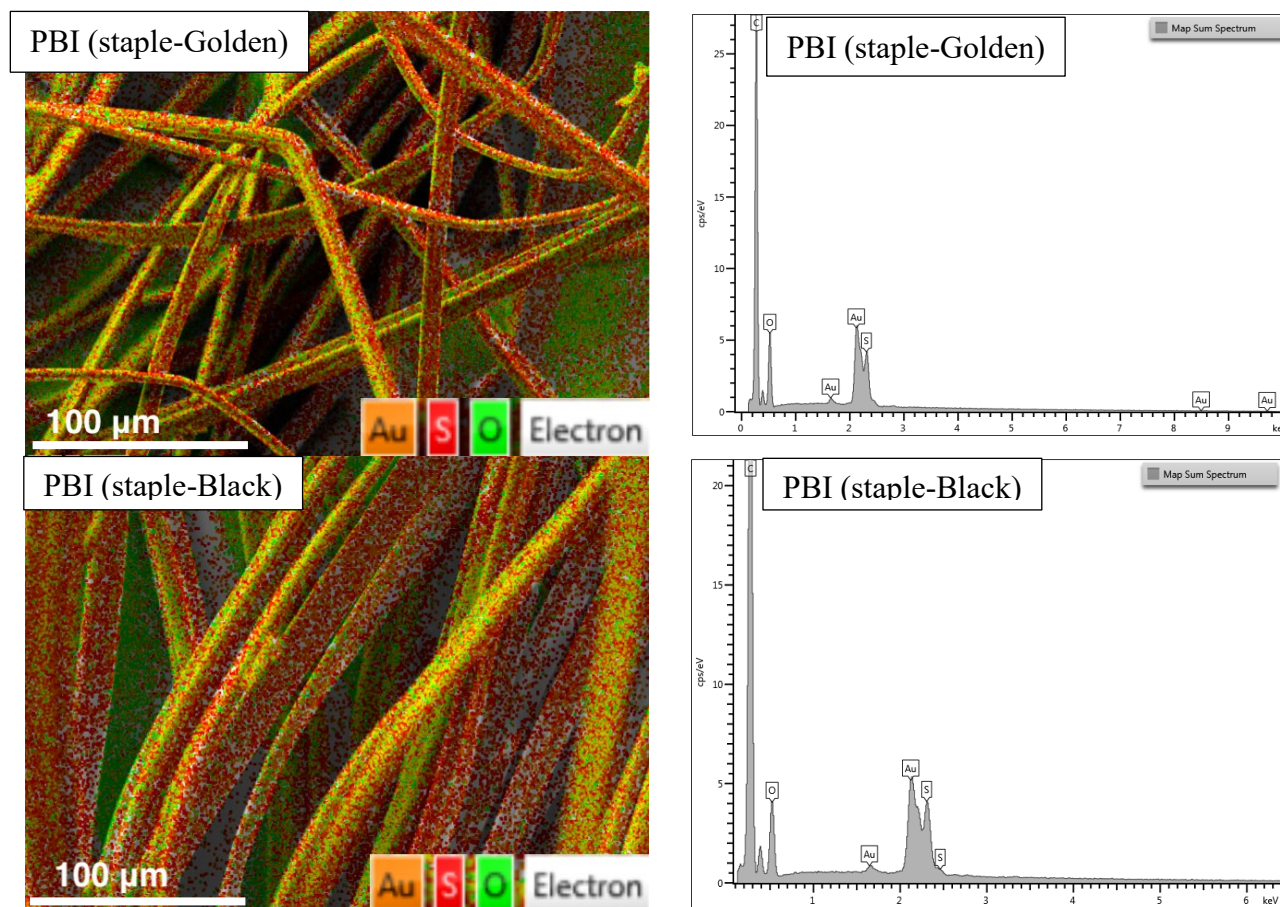| Spectrum No.	Sulfur content (atm.%)	Average Sulfur (atm.%)
Filament yarn (p-aramid) areas		
7	0.32	
8	0.41	
9	0.27	
10	0.41	
11	0.26	
12	0.29	0.37 ± 0.05
22	0.33	
23	0.32	
24	0.29	
27	0.27	
28	0.25	
29	0.28	
Spun yarn (p-aramid & PBI) areas		
2	0.99	
3	1.81	
4	1.24	
5	1.19	
6	1.40	
13	1.20	
14	1.47	1.3 ± 0.2
15	1.04	
16	1.33	
17	1.44	
18	1.69	
19	1.19	
20	1.41	
21	1.02	

Table 3: Sulfur content in specific areas corresponding to the spun yarns and filament yarns for Fabric MC in the unaged condition (areas circled in red correspond to para-aramid filament yarns and areas in green to para-aramid/meta-aramid spun yarns).

Spectrum No.	Sulfur content (atm.%)	Average Sulfur (atm.%)
Filament yarn (p-aramid) areas		
2	0.23	
3	0.24	
4	0.26	
5	0.31	
6	0.23	0.29 ± 0.06
10	0.24	
11	0.37	
12	0.31	
16	0.39	
Spun yarn (p-aramid & m-aramid) areas		
7	0.07	
8	0.17	
13	0.11	0.23 ± 0.05
14	0.19	
15	0.10	

EDX spectra were also collected on individual bundles of as-received para-aramid, meta-aramid and PBI fibers provided by their respective manufacturers. Both staple fibres and filaments were analyzed in the case of para-aramid, whereas EDX analyses on meta-aramid and PBI were only performed on staple fibers. PBI staple fibers were obtained in two types: golden and black. **Figure 10** shows a representative EDX layered image of each of these fibers, as well as the corresponding EDX spectra listing the different elements identified.

p-aramid (staple)

Au S Na O Electron

100 µm

p-aramid (staple)

Map Sum Spectrum

p-aramid (filament)

Au S Na O Electron

100 µm

p-aramid (filament)

Map Sum Spectrum

m-aramid (staple)

Au K O Electron

100 µm

m-aramid (staple)

Spectrum 9

Figure 10: Example of EDX layered image and spectrum for para-aramid, meta-aramid and PBI fibers and filaments (sulfur appears in red in the EDX images).

The sulfur content (atomic %) found in staple and filament para-aramid fibers was 0.24 and 0.25, respectively, which is close to the sulfur content found in areas corresponding to para-aramid filament yarns (0.37 ± 0.05) in Fabric MH. On the other hand, a large amount of sulfur was found in both the golden and black types of PBI fibers; it was 3.26 and 3.58, respectively. Interestingly, the amount of 1.30 % of sulfur in areas corresponding to the para-aramid/PBI spun yarns in Fabric MH is situated between the amounts found in the para-aramid and PBI fibers analyzed individually. Finally, no sulfur was found in the meta-aramid staple fibers, which is in agreement with the results of the EDX analysis of Fabric MF, which contains 93% meta-aramid staple fibers.

The EDX analysis was also performed on the yarn cross-sections prepared by cutting them with a pair of cut-resistant fabric scissors. As shown in **Figure 11** for para-aramid/PBI yarns, sulfur was found throughout the cross-section of the fibers.
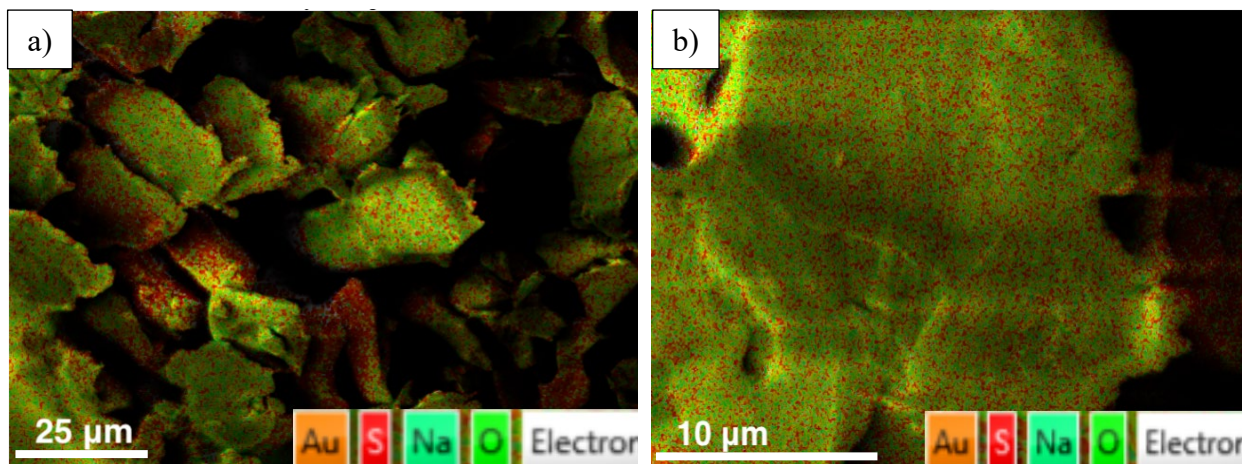
Figure 11: EDX analysis of the cross-section of para-aramid/PBI yarn- a) bundle of para-aramid/PBI fibers, b) single fiber.

Figure 12 shows the pH values of the RO water collected from the flasks after 50 days of hydrothermally aging of the different fabrics at 90°C. The pH of the RO water originally used for the hydrothermal aging (labelled as Blank) is also included for comparison purposes. The RO water corresponding to the Blank condition showed a neutral pH (7.33). After 50 days of aging at 90°C, the RO water in the flasks containing the Group 1 fabrics (MA, MB, MG, MH) became acidic, with pH values ranging between 3.23 and 3.75. On the other hand, the aging water of all the Group 2 fabrics (MC, MD, ME, MF) had become slightly basic after 50 days of aging at 90°C, with pH values between 8.26 and 8.74.
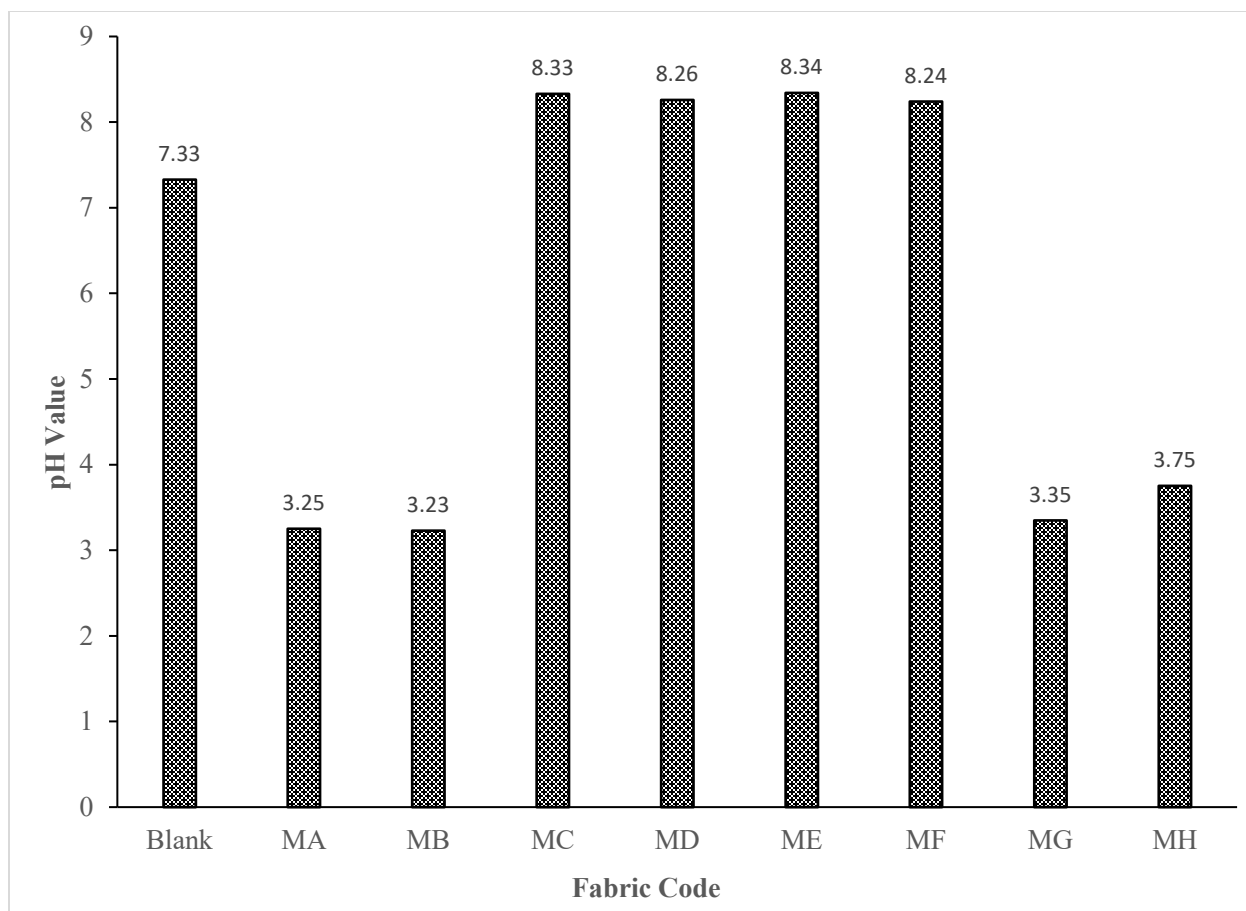
Figure 12: pH values of the original RO water (labelled as Blank) and after 50 days of

hydrothermal aging (90°C) of the different fabrics.

3.3. Surface Condition Analysis
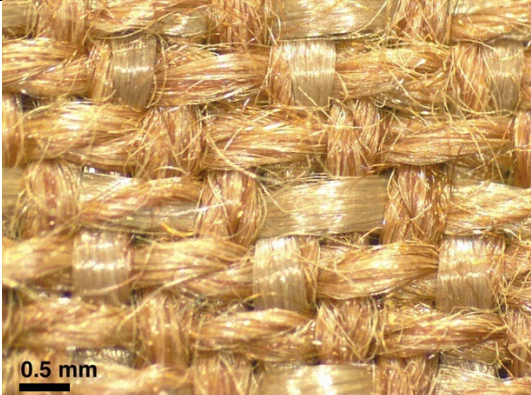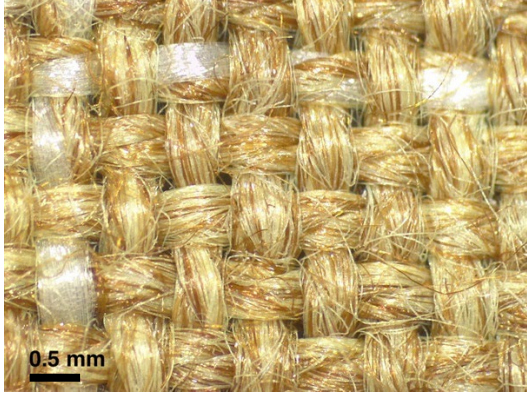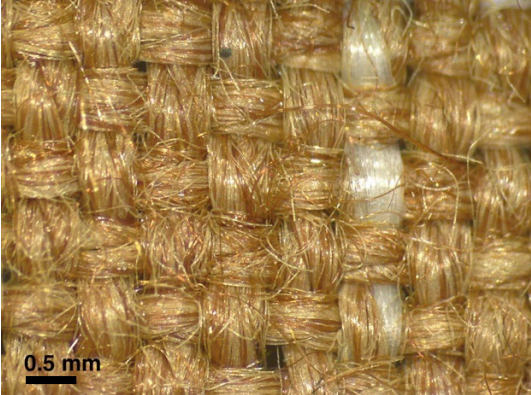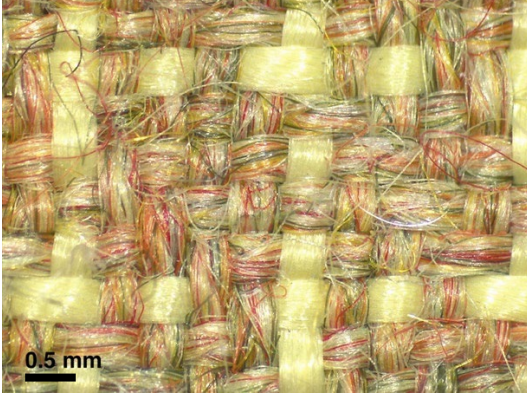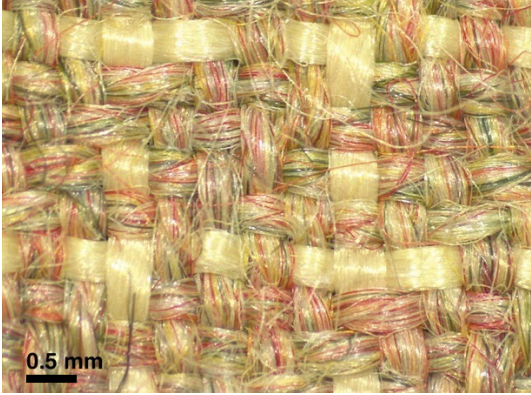
The surface condition of the eight fabrics after the hydrothermal aging was analyzed by optical

microscopy, SEM, water contact angle measurements, and liquid absorbency capacity test.

3.3.1. Surface Morphological Analysis

The surface of each fabric, both in the unaged and aged conditions, was observed by optical

microscopy and SEM. SEM observations were performed at different magnifications between 40X

and 1000X. Representative examples of microscopy images of the unaged and aged specimens are

given in Table 4, while Table S2 (in Supporting Information) provides SEM images of the unaged

and aged specimens at the fabric and fiber scale.

Table 4: Optical microscopy images of unaged and hydrothermally aged specimens of the eight

fabrics.

Fabric Code	Optical Microscopy Images	
	Unaged	Aged at 90°C for 50 Days
MA		
MB		
MC		

MD		
ME		
MF		
MG		

| MH | | |
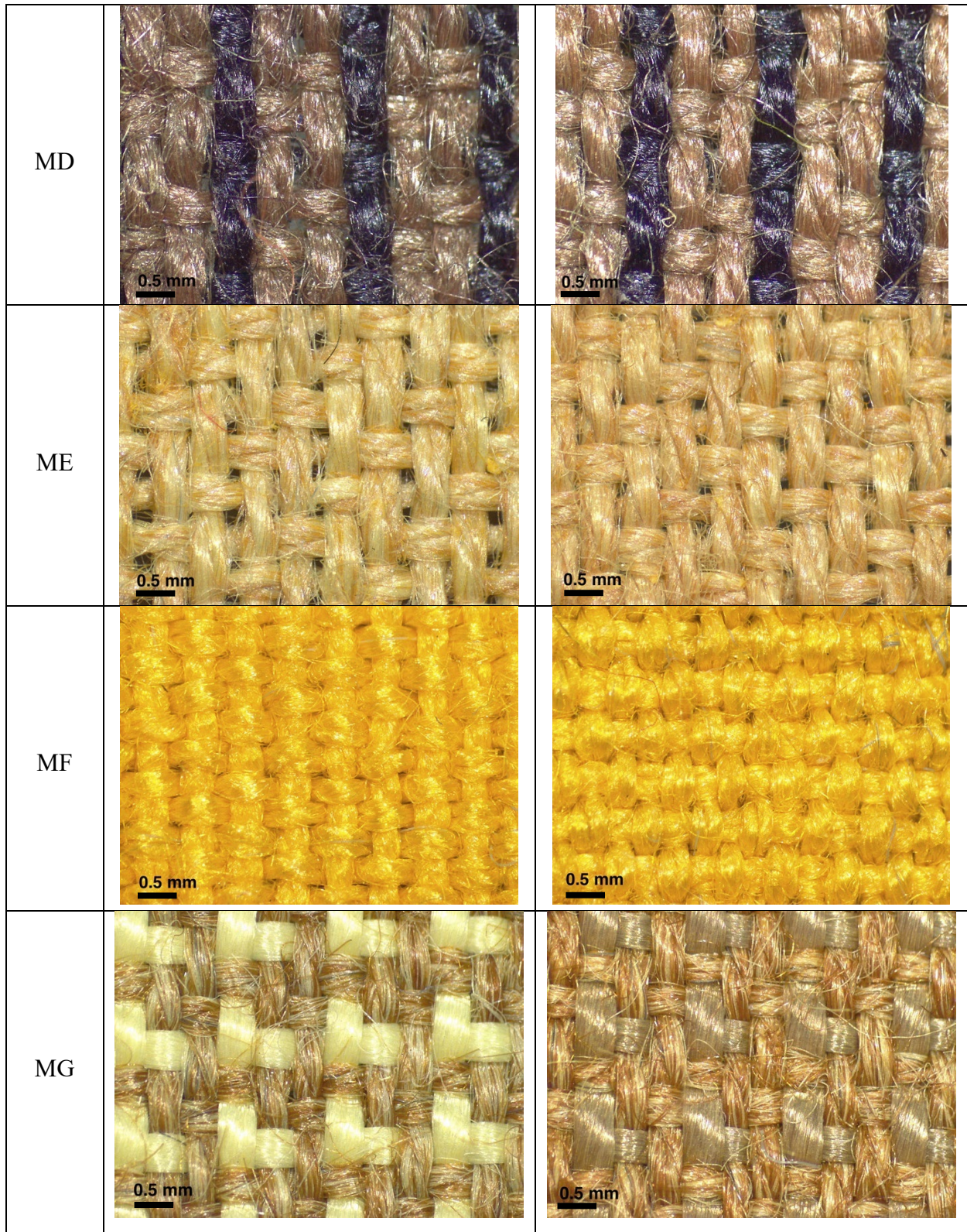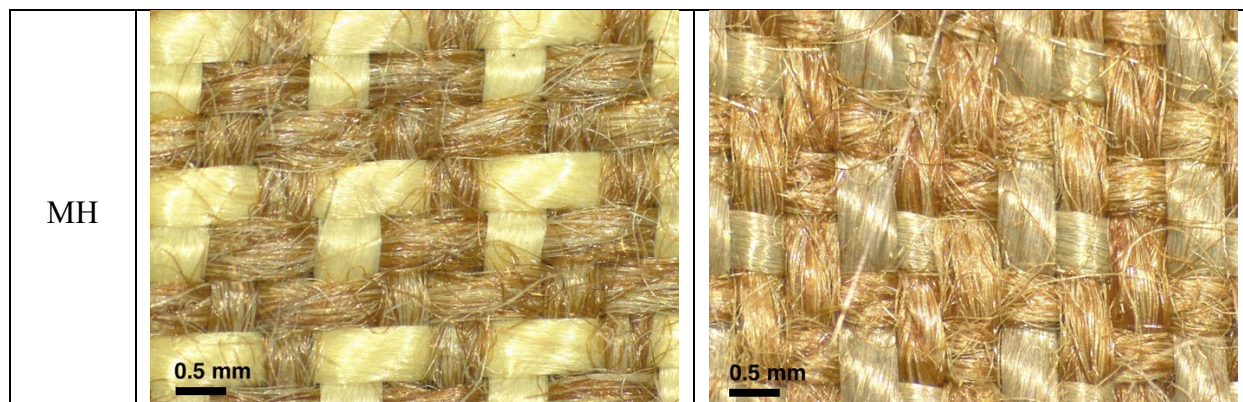
Obvious changes in the color of the specimens after hydrothermal aging can be observed in Fabric MA, MB, MG, and MH on the microscopy images in Table 4. Slight changes in the color were also observed for Fabric ME, while no distinguishable changes in color were observed in Fabric MC, MD and MF. On the other hand, no change in the microstructure was obvious in any of the hydrothermally aged specimens.

Similar to the optical microscopy observations, no morphological changes between the unaged and aged conditions were observed in the SEM images (Table S2 in supporting information) both at magnification x40 (fabric scale) and x200 (fiber scale). A similar absence of modification in the surface morphology of fibers following hydrothermal aging was also reported by Li et al. in the case of para-aramid fibers.[29]

3.3.2. Water Contact Angle

The water contact angle of the fabrics was assessed to evidence any potential effect of the hydrothermal aging on their water repellent finish. For this purpose, the water contact angle of the fabrics was measured for both unaged and aged specimens. The results are shown in **Figure 13**.
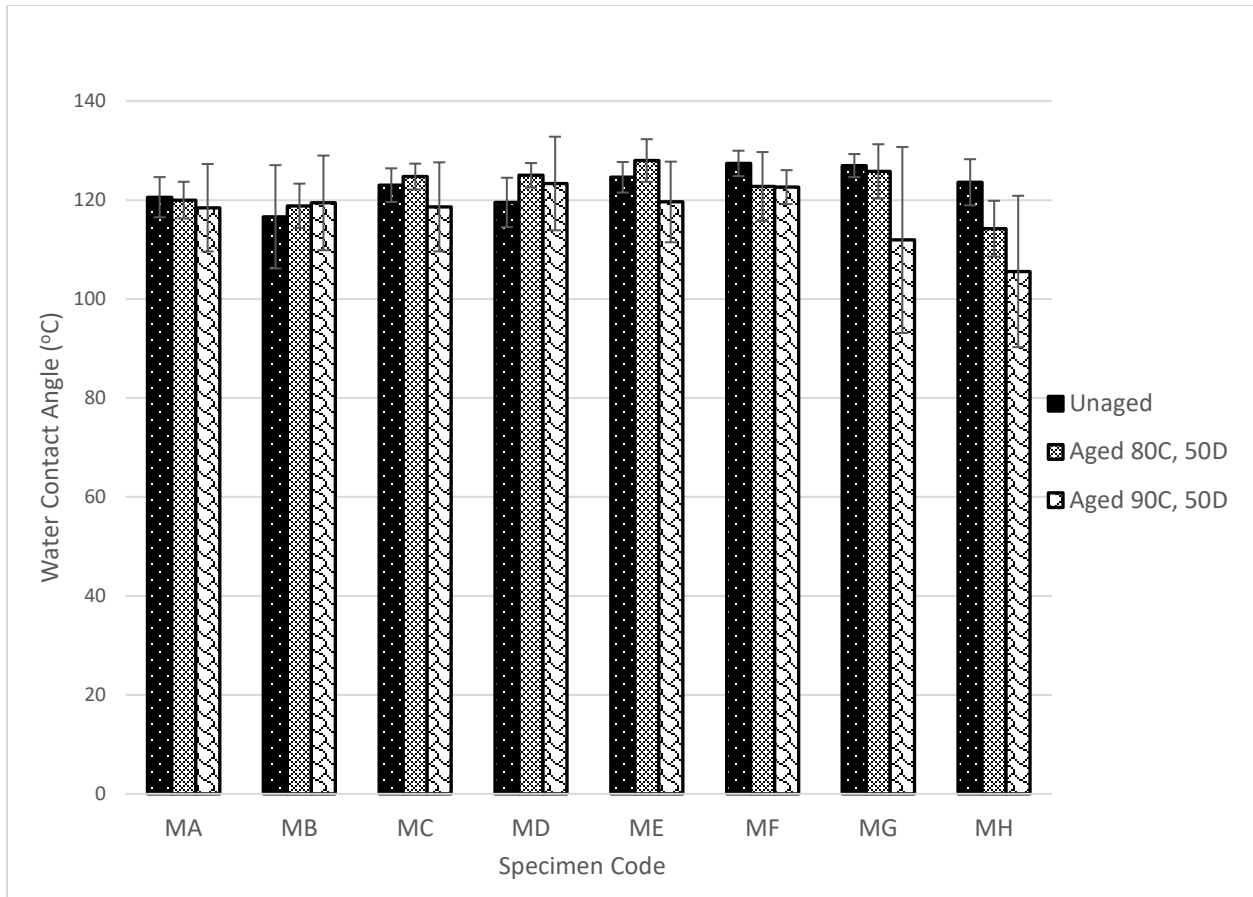
Figure 13: Water contact angle results for unaged specimens and specimens hydrothermally aged for 50 days at temperatures of 80 and 90°C.

Fabric MH showed a significant difference between the unaged and aged specimens ($p = 0.014$ for the aged condition at 80°C for 50 days and $p = 0.031$ for the aged condition at 90°C for 50 days). This finding may potentially indicate the degradation of the water repellent finish of Fabric MH because of hydrothermal aging. In the case of Fabric MG, although it was not statistically significant ($p = 0.299$ for the aged condition at 80°C for 50 days and $p = 0.079$ for the aged condition at 90°C for 50 days) due to the large variability in the results, a difference in the water contact angle can be observed for the condition corresponding to 50 days of aging at 90°C compared to the other conditions. On the other hand, no significant differences in the water contact

angle between the unaged and aged specimens were observed for the rest of the fabrics. In general, the variability in the contact angle results is relatively high, which can be associated with the high roughness of the fabrics.

3.3.3. Liquid Absorbency Capacity

LAC measurements were also conducted to complement the identification of potential effects of the hydrothermal aging on the fabric water repellent finish. The results of the LAC test are shown in **Figure 14**.
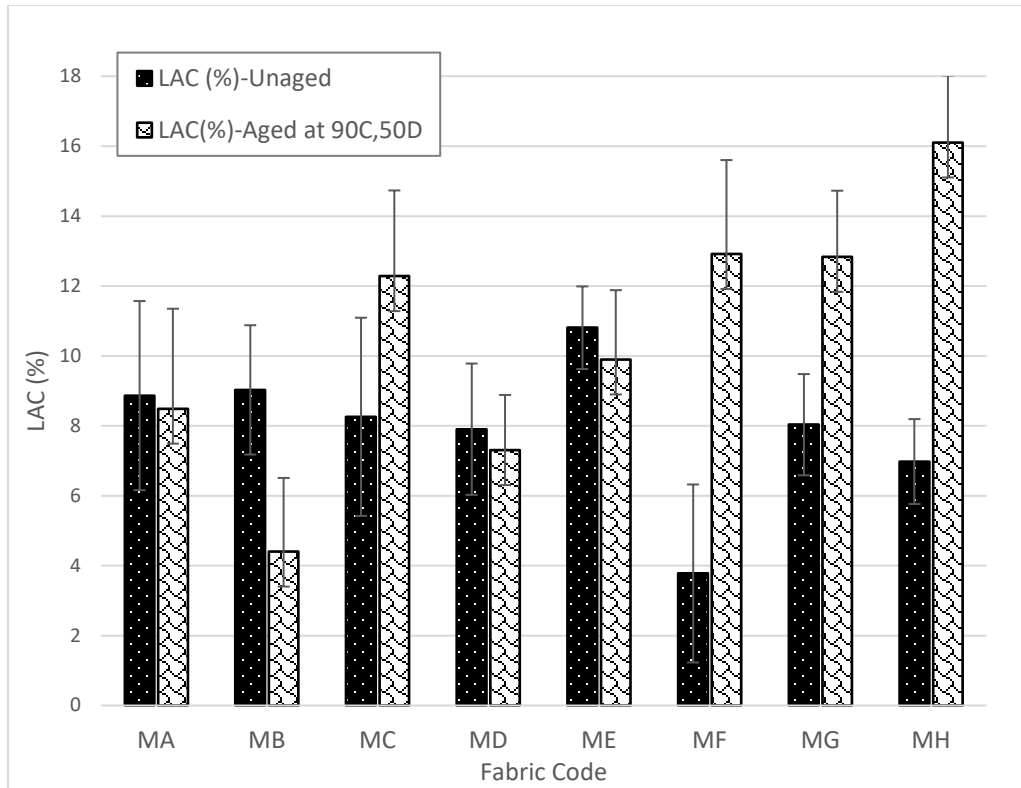
Figure 14: Liquid absorbency capacity measured on unaged specimens and specimens hydrothermally aged at 90°C for 50 days.

Fabric MB (p=0.004), MF (p=0.002), MG (p=0.004), and MH (p=0.000) showed significant differences between the LAC results for the unaged specimens and the specimens hydrothermally

aged at 90°C for 50 days. In the case of Fabric MH and MG, these observations are in agreement with the results of the water contact angle measurements. The degradation of the water repellent finish evidenced by the change in the water contact angle with hydrothermal aging thus leads to an increased water absorbance by the fabric.

In the case of Fabric MF, a large increase in the water absorbency is observed as a result of hydrothermal aging, while no difference in the water contact angle was recorded. A change in the fabric hand feel was also noted after 50 days of thermal aging at 90°C. While the fabric was initially stiff, it became more flexible after hydrothermal aging. Both this change in the fabric stiffness and the increase in the water absorbency point towards a degradation of the water repellent finish as a result of hydrothermal aging. For Fabric MC, even if the change in water absorbency was not statistically significant in that case (p=0.106), a similar change in the fabric stiffness after hydrothermal aging also points towards a degradation of the water repellent finish as a result of hydrothermal aging.

Finally, an opposite behavior was observed with Fabric MB. Its liquid absorbency capacity reduced significantly after hydrothermal aging.

4. Discussion

Among the eight different fabrics tested, some of them experienced large drops in tensile strength after hydrothermal aging, including at temperatures as low as 60°C (**Figure 3 and 7**). For instance, two para-aramid/PBI fabrics (MA and MB) lost more than 50% of their strength after 50 days of hydrothermal aging at 60°C, and two others (MG and MH) lost between 40 and 50% of strength

in the same conditions. This observation is a concern for the safety of firefighters as 60°C is considered the upper limit of their routine operating conditions.[45]

A comparison between the residual breaking force results for Group 1 and Group 2 fabrics shows that fabrics containing para-aramid/PBI fibers appear to be more sensitive to hydrothermal aging than fabrics containing meta-aramid fibers. While all the Group 1 fabrics lost more than 40% of their strength after 50 days of hydrothermal aging at 60°C (**Figure 4**), none of the Group 2 fabrics experienced any strength loss at that temperature (**Figure 8**). Similarly, the strength of Group 1 fabrics decreased by 55 to 75% after 50 days of hydrothermal aging at 90°C, whereas only two of the Group 2 fabrics showed a significant decrease in strength in the same conditions, by 45% for Fabric MD and 20% for Fabric ME. Interestingly, none of the eight fabrics showed any changes in their microstructure as observed by SEM (**Table S2**), even when the fabric's force at the break had dropped by 75% after 50 days of hydrothermal aging at 90°C (Fabric MA). These reductions in the fabric strength after hydrothermal aging are in agreement with data published on the effect of repeated launderings on the tearing strength of seven fire-protective fabrics of similar fiber contents.[32] This larger loss in the force at break with hydrothermal aging for para-aramid/PBI fabrics may be attributed to the fact that para-aramid fibers are known to be sensitive to hydrolysis in the presence of an acid catalyst.[22] The large effect of hydrothermal aging on para-aramid/PBI fabrics observed here is also in agreement with what has been reported in the literature for a para-aramid/PBI fabric exposed to atmospheric moisture.[22]

However, Fabric MC has a similar para-aramid fiber content as Fabric MA, MH, and MG (**Table 1**). Nevertheless, Fabric MC did not experience any significant reduction in its strength after

hydrothermal aging (**Figure 7**), while the mechanical performance of Fabric MA, MG, and MH was largely affected (**Figure 3**). The difference between Fabric MC and the three other fabrics is that the complement to the para-aramid fibers in Fabric MC is meta-aramid, while the complement to the para-aramid fibers in Fabric MA, MH, and MG is PBI. If meta-aramid fibers have been reported to be less affected by hydrothermal aging compared to para-aramid fibers due to their closer packing preventing easy water ingress into the polymer network[43] and the similar structure of their core and skin avoiding localized core degradation [21], PBI fibers are not expected either to be sensitive to hydrolysis because of the entirely aromatic structure of the polymer molecule.[22]

The reason for this difference in behavior may lie in the sulfur content of the different fibers. Sulfuric acid is used in the spinning process of all three types of fibers involved, para-aramid [46], meta-aramid [47], and PBI [44]. However, large differences in the sulfur content between these fibers were observed at the fabric (**Figure 9**), yarn (**Table 2** and **3**), and fiber (**Figure 10**) levels. For instance, a very little amount of sulfur was detected in Fabric MC ($0.33 \pm 0.01\%$), while the sulfur content was $2.8 \pm 0.2\%$, $2.8 \pm 0.4\%$, and $2.2 \pm 0.3\%$ for Fabric MA, MG, and MH, respectively. At the yarn scale, the para-aramid/meta-aramid spun yarns in Fabric MC showed a sulfur content of 0.23 ± 0.05 %, while the para-aramid/PBI spun yarns in Fabric MH showed a sulfur content of 1.3 ± 0.2 %. Finally, at the fiber level, the sulfur content in para-aramid fibers was 0.24%, while it was 3.3% and 3.6% in the golden and black PBI fibers, respectively. These results provide a strong indication that the larger decrease in tensile strength observed in the para-aramid/PBI fabrics as a result of hydrothermal aging can potentially be associated with the larger residual sulfur content in the PBI fibers compared to meta-aramid fibers.

Furthermore, all the Group 2 fabrics showed a very limited amount of sulfur. It is 0.31% in Fabric MC, 0.39% in Fabric MD, and 0.30% in Fabric ME, while no traces of sulfur were detected for Fabric MF. Group 2 fabrics displayed better resistance to hydrothermal aging conditions compared to Group 1 fabrics. This finding strengthens the hypothesis of the contribution of the residual sulfur from the spinning process in accelerating the hydrothermal aging behavior of some of the fire-protective fabrics tested.

A further confirmation of the impact of the residual sulfur in the PBI fibers on the hydrothermal aging of the para-aramid fibers can be found in the values of the pH (**Figure 12**) of the aging water measured after 50 days of aging at 90°C. While the hydrothermal aging water of the Group 2 fabrics, which do not contain PBI fibers, only showed a slight increase in the pH, the aging water of the Group 1 fabrics, i.e., containing PBI fibers, had become strongly acidic after 50 days of aging at 90°C. The acidic nature of the aging water resulting from sulfur leaching out of the PBI fibers during the aging process accelerates the degradation of the para-aramid fibers in comparison to the slightly basic water experienced by the Group 2 fabrics. The large reduction in the Group 1 fabrics' mechanical strength as a result of the hydrothermal aging can thus be directly attributed to the large amounts of residual sulfur in the PBI fibers after the fiber manufacturing process.

In the case of Group 2 Fabric MD and ME, they both contain the same para-aramid content (60%) and have a similar fabric structure, mass, thickness, fabric count, and yarn type. However, the complement to the para-aramid fibers in Fabric MD is meta-aramid fibers (40%), while in Fabric ME, 20% of the fiber content is meta-aramid, and 20% is PBO fibers. Both fabrics saw their strength decrease as a result of hydrothermal aging. However, Fabric MD was more strongly

affected. Since the presence of PBO fibers in the fiber content seems to be the only major difference between Fabric MD and ME, it can potentially be attributed as the reason for the better resistance of Fabric ME to hydrothermal aging. A good resistance to repeated domestic launderings was also reported for a fabric with a similar content as Fabric ME compared to other para-aramid-containing outer shell fire-protective fabrics.[32] On the other hand, PBO has been reported as sensitive to atmospheric moisture in previous studies.[48] This may indicate a difference in the aging behavior of PBO fibers between water immersion and exposure to atmospheric moisture.

Another effect of hydrothermal aging on the fire-protective fabric performance was observed in terms of water repellency. For instance, Fabric MG and MH exhibited a reduced water contact angle (**Figure 13**) and increased water absorbency capacity (**Figure 14**) after 50 days of hydrothermal aging at 90°C. For Fabric MF, there was also a large increase in water absorbency but no significant change in the water contact angle. This finding indicates that hydrothermal aging has the potential to degrade water repellent finishes. In addition, the results show that the measurement of the liquid absorbency capacity appears to be a more reliable indicator of the effect of hydrothermal aging on the water repellent finish compared to water contact angle measurements.

5. Conclusion

This study investigates the effect of a generally unnoticed hazard, i.e., hydrothermal conditions, on the mechanical performance and water repellency of eight fire-protective fabrics of different fiber contents. A larger loss in the fabric strength was observed for the para-aramid/PBI-based

fabrics studied compared to the meta-aramid-containing fabrics. It was attributed to the higher sensitivity of para-aramid fibers to hydrolysis compared to meta-aramid fibers. Furthermore, EDX analysis revealed a higher amount of sulfur in the para-aramid/PBI-based fabrics, which was mainly attributed to the PBI fibers. This larger amount of sulfur in the para-aramid/PBI fabrics, which is possibly a residue of the PBI fiber spinning process, is believed to be responsible for the larger loss in the mechanical performance observed in the para-aramid/PBI fabrics when exposed to hydrothermal aging, leading to an accelerated hydrolysis of the para-aramid fibers in acidic conditions.

On the other hand, no morphological changes were observed at the microscopic level, even for the fabrics exhibiting a large loss in mechanical performance after exposure to hydrothermal aging. For their part, the water contact angle and liquid absorbency capacity test results hint toward a degradation of the water-repellent finish for some fabrics as a result of hydrothermal aging. A more or less pronounced change in the fabric color was also observed in some instances.

These results provide some breakthrough information regarding the possible reason for the larger reduction in the mechanical performance of para-aramid/PBI fabrics when exposed to a combination of water and temperature. They also demonstrate the need for more research in the area of high-performance fabric aging as well as the development of tools to predict and monitor their long-term performance.

Supporting Information

Supporting Information is available from the Wiley Online Library.

Acknowledgments

Conflicts of Interest

The authors declare no conflict of interest

References

[1]   S. Mandal, S. Gaan, M. Camenzind, S. Annaheim, and R. M. Rossi, in *Thermal Analysis of Textiles and Fibers*, Vol. 1 (Eds: Michael J. and Joseph M.) Woodhead Publishing, Cambridge, UK **2020**, Ch. 21.

[2]   P. Bajaj, *Bull. Mater. Sci.*, **1992**, 15, 67

[3]   G. Song and F. Wang, *Firefighters' clothing and equipment: Performance, protection and comfort*, CRC Press, Boca Raton, US **2018.**

[4]   F. S. Kilinc, *Handbook of fire resistant textiles*. Woodhead Publishing, Cambridge, UK, **2013.**

[5]   A. R. Horrocks, in *Handbook of Technical Textiles*, Vol. 2 (Eds: A. Richard Horrocks and Subhash C. A.) Woodhead Publishing, Cambridge, UK **2016,** Ch. 8.

[6]   A. Hassanin, *Ph.D. Thesis,* North Carolina State University, **2011.**

[7]   H. Murase and K. Yabuki, in *High-Performance and Specialty Fibers: Concepts, Technology and Modern Applications of Man-Made Fibers for the Future*, Vol.1 (Eds: Japan The Society of Fiber Science and Techno) Springer, Tokyo, Japan, **2016**, Ch. 5.

[8]   S. Bourbigot and X. Flambard, *Fire Mater.*, **2002**, 26, 155.

[9]   H. G. Chae and S. Kumar, *J. Appl. Polym. Sci.*, **2006**, 100, 791.

[10]   Shaid Abu, Wang Lijing, and Padhye Rajiv, in *Firefighters' Clothing and Equipment: Performance, Protection, and Comfort*, Vol. 1(Eds: G. Song and F. Wang) CRC Press, Boca Raton, US **2018**, Ch. 1.

[11]   M. McQuerry, S. Klausing, D. Cotterill, and E. Easter, *Fire Technol.*, **2015**, 51, 1149.

[12]   T. L. Vogelpohl and E. Easter, *Master Thesis,* University of Kentucky, **1996.**

[13]   D. G. Cotterill, *Master Thesis,* University of Kentucky, **2009.**

[14]   S. L. Trenkamp, *Masters Thesis,* University of Kentucky, **2011.**

[15]   M. L. Cinnamon, *Masters Thesis,* University of Kentucky, **2013.**

[16]   NFPA 1971, Standard on protective ensemble for structural fire fighting and proximity fire fighting, National Fire Protection Association, Quincy, Massachusetts, **2018**.

[17]   C. Arrieta, E. David, P. Dolez, and V. K. Toan, *J. Appl. Polym. Sci.*, **2010**, 115, 3031.

[18]   C. Arrieta, E. David, P. Dolez, and T. Vu-Khanh, *Polym. Compos.*, **2011**, 32, 362.

[19]   P. I. Dolez, N. S. Tomer, and Y. Malajati, *J. Appl. Polym. Sci.*, **2019**, 136, 47075.

[20]   M. Rezazadeh and D. A. Torvi, *Fire Technol.*, **2011**, 47, 565.

[21]   S. Houshyar, R. Padhye, S. Ranjan, S. Tew, and R. Nayak, *J. Ind. Text.*, **2018**, 48, 77.

[22]   C. Arrieta, É. David, P. Dolez, and T. Vu-Khanh, *Polym. Degrad. Stab.*, **2011,** 96, 1411.

[23]   R. L. Barker, presented at *National Personal Protection Technology Laboratory, National Institute for Occupational Safety and Health (NIOSH),* Pittsburgh, Pennsylvania, January 31, **2005.**

[24]   S. Mandal, M. Camenzind, S. Annaheim, and R. M. Rossi, in *Advanced Characterization and Testing of Textiles*, Vol. 1. (Eds: P. Dolez, O. Vermeersch, and V. Izquierdo) Woodhead Publishing, Cambridge, UK **2018**, Ch. 9.

[25]   K. Saijo, O. Arimoto, T. Hashimoto, M. Fukuda, and H. Kawai, *Polymer (Guildf).*, **1994**, 35, 496.

[26]   M. Fukuda, M. Ochi, M. Miyagawa, and H. Kawai, *Text. Res. J.*, **1991**, 61, 668.

[27]   K. Slater, *Text. Prog.*, **1991**, 21, 1.

[28]   A. Engelbrecht-Wiggans, F. Burni, E. Guigues, S. Jiang, TQ. Huynh, Z. Tsinas, D. Jacobs, AL. Forster, *Text. Res. J.*, **2020,** 90, 2428.

[29] C. S. Li, M. S. Zhan, X. C. Huang, and H. Zhou, *J. Appl. Polym. Sci.*, **2012**, 126, 552.

[30] J. Chin, A. Forster, C. Clerici, L. Sung, M. Oudina, and K. Rice, *Polym. Degrad. Stab.* **2007**, 92, 1234.

[31] NFPA 1851, Standard on selection, care, and maintenance of protective ensembles for structural fire fighting and proximity fire fighting. National Fire Protection Association, Quincy, Massachusetts, **2020**.

[32] P. I. Dolez and Y. Malajati, in *Performance of Protective Clothing and Equipment: Innovative Solutions to Evolving Challenges*, Vol. 11. (Eds: K. Lehtonen, B. P. Shiels, and R. B. Ormond) ASTM International Committee F23, West Conshohocken, USA, September **2020**.

[33] H. Makinen, in *Performance of Protective Clothing*, **1992,** 4, 754.

[34] S. Nazaré, S. Flynn, R. Davis, and J. Chin, *Fire Technol.*, **2014,** 50, 1301.

[35] D. N. Yehia, *Master Thesis,* University of Alberta, **2021.**

[36] A. Saha, *Master Thesis,* University of Alberta, **2021.**

[37] ASTM D5035-11, Standard Test Method for Breaking Force and Elongation of Textile Fabrics (Strip Method), American Society for Testing and Materials, West Conshohocken, Pennsylvania, **2019.**

[38] CAN/CGSB-4.2.No./N°2-M88, Textile Test Methods Conditioning Textile Materials for Testing, Canadian General Standards Board, Ottawa, **2013.**

[39] M. Van Gurp and J. Palmen, *Rheol. Bull.*, **1998**, 67, 5.

[40] A. Plota and A. Masek, *Materials (Basel).*, **2020,** 13, 4507.

[41] ISO 9073-6, Textiles-Test methods for nonwovens-Part 6: Absorption 5. Liquid absorption capacity (EN 29073 part 6), International Organization for Standardization, Vernier, Geneva, **2000.**

[42] R. J. Morgan and N. L. Butler, *Polym. Bull.*, **1992**, 27, 689.

[43] E. Galli, *Plast Compd.*, **1981**, 4, 21.

[44] A. R. Horrocks, H. Eichhorn, H. Schwaenke, N. Saville, C. Thomas, in *High-performance Fibers,* Vol. 1. (Eds: J.W.S. Hearle) Woodhead Publishing and CRC Press, **2001**, Ch. 9.

[45] R. Rossi, *Ergonomics*, **2003**, 46, 1017–1033.

[46] S. Rebouillat, in *High-performance fibres*, Vol. 1. (Eds: J.W.S. Hearle) Woodhead Publishing and CRC Press, **2001**, Ch. 2.

[47] B. L. Deopura and N. V. Padaki, in *Text. Fash. Mater. Des. Technol.*, Vol. 1. (Eds: R. Sinclair) Woodhead Publishing Cambridge, UK **2015**, Ch. 5.

[48] A. L. Forster, D. D. Leber, A. Engelbrecht-Wiggans, V. Landais, A. Chang, E. Guigues, G. Messin, M. A. Riley, *J. Res. Natl. Inst. Stand. Technol*, **2020**, 125, 125026.

Supporting Information

Table S1: Number of yarns in the ravelled specimens for each fabric.

Fabric Code	Number of yarns in the specimens after ravelling
MA	46 (16 filament yarns + 30 spun yarns)
MB	36 (6 filament yarns + 35 spun yarns)
MC	61 (13 filament yarns + 48 spun yarns)
MD	46 (16 filament yarns + 30 spun yarns)
ME	45 (All spun yarns)
MF	67 (All spun yarns)
MG	61 (21 filament yarns + 40 spun yarns)
MH	46 (16 filament yarns + 30 spun yarns)

Table S2: SEM images of unaged and hydrothermally aged specimens of eight fabrics.

Fabric Code	SEM Images	
	Unaged	Aged at 90°C for 50 Days
MA		

MB		
MC		

200 µm / 30 µm / 200 µm / 20 µm

51

MD		
ME		

MF		
MG		

MH	 200 μm 200 μm 20 μm 20 μm